
High-order Interactions Modeling for Interpretable Multi-Agent Q-Learning

Qinyu Xu

School of Management and Engineering
Nanjing University
qinyuxu@smail.nju.edu.cn

Yuanyang Zhu[†]

School of Information Management
Nanjing University
yuanyangzhu@nju.edu.cn

Xuefei Wu[†]

School of Management and Engineering
Nanjing University
xuefeiwu@smail.nju.edu.cn

Chunlin Chen

School of Robotics and Automation
Nanjing University
clchen@nju.edu.cn

Abstract

The ability to model interactions among agents is crucial for effective coordination and understanding their cooperation mechanisms in multi-agent reinforcement learning (MARL). However, previous efforts to model high-order interactions have been primarily hindered by the combinatorial explosion or the opaque nature of their black-box network structures. In this paper, we propose a novel value decomposition framework, called Continued Fraction Q-Learning (QCoFr), which can flexibly capture arbitrary-order agent interactions with only linear complexity $\mathcal{O}(n)$ in the number of agents, thus avoiding the combinatorial explosion when modeling rich cooperation. Furthermore, we introduce the variational information bottleneck to extract latent information for estimating credits. This latent information helps agents filter out noisy interactions, thereby significantly enhancing both cooperation and interpretability. Extensive experiments demonstrate that QCoFr not only consistently achieves better performance but also provides interpretability that aligns with our theoretical analysis.

1 Introduction

Cooperative multi-agent reinforcement learning (MARL) has recently drawn much attention [1], such as autonomous vehicles [2, 3, 4], robotics [5, 6], and autonomous warehouses [7, 8]. Success in these domains generally depends on a tapestry of local interactions: agents influence one another not only through explicit pairwise effects but also through higher-order dependencies that shape emergent behaviour [9, 10], which is a key factor to make coordination efficient. How to model those interactions among agents and to do so in a way humans can understand remains a challenge.

Value decomposition MARL has emerged as a powerful framework with the large capacity of deep neural networks and the centralized training and decentralized execution (CTDE) paradigm, which factorises a team return into individual utilities. Leading value decomposition models—such as the monotonic mixer in QMIX [11]—capture interaction structure only implicitly, leaving their decisions opaque. Post-hoc explainers (e.g., Shapley value attribution [12] and masked-attention visualisation [13]) offer limited insight and could not recover the underlying temporal or relational dynamics. Another inherent interpretable technique, like decision tree [14, 15, 16] or Shapley-based [12], handles only low-order interactions; higher-order terms still explode combinatorially.

[†]Corresponding author: Yuanyang Zhu and Xuefei Wu.

Here, we argue that modeling high-order collaboration patterns among agents is still crucial for promoting coordination, which is still missing. Continued fractions [17, 18] provide a natural remedy: their recursive form captures interactions of any order, and a simple truncation yields a finite and interpretable approximation without combinatorial blow-up.

Building on these ideas, we propose Continued Fraction Q-Learning (QCoFr), a novel framework that combines expressive value decomposition with intrinsic interpretability. QCoFr represents the joint action-value function as a weighted sum of continued fraction modules—recursive structures that explicitly approximate arbitrary-order interactions among agents with linear complexity $\mathcal{O}(n)$ in the number of agents. To strengthen credit assignment, QCoFr incorporates a variational information bottleneck (VIB) [19] to capture task-relevant latent information to bridge local histories to the optimal joint action \mathbf{u} . The assistive information will be used to estimate the credits together with global state s for assisted value factorization, which relieves the spurious correlation between state s and Q_{tot} . We also give a rigorous proof that QCoFr takes a linear combination of continued fractions and has the property of universal approximation, even each with finite depth and linear layers. We demonstrate through extensive experiments on LBF, SMAC, and SMACv2 benchmarks that QCoFr not only generally achieves better performances on solving all tasks but also provides interpretability lacking in the state-of-the-art baselines.

2 Background

Dec-POMDP. A fully cooperative multi-agent task can be modeled as a Decentralized Partially Observable Markov Decision Process (Dec-POMDP) [20]. A Dec-POMDP can be defined as a tuple $\langle N, S, U, P, r, Z, O, n, \gamma \rangle$, where N denotes a set of n agents and $s \in S$ is the global state of the environment. At each time step, agent i selects an action $u_i \in U$, forming a joint action $\mathbf{u}_t \in \mathbf{U} \equiv U^n$. This results in the next state s' according to the state transition function $P(s' | s, \mathbf{u}) : S \times \mathbf{U} \times S \rightarrow [0, 1]$. All agents obtain the same joint reward $r(s, \mathbf{u}) : S \times U^n \rightarrow \mathbb{R}$ and $\gamma \in (0, 1]$ is the discount factor. Due to partial observability, each agent $i \in N$ receives individual observation $z_i \in Z$ from observation function $o_i \in O(s, i)$. Each agent maintains an action-observation history $\tau_i \in T$, conditioned by its policy π_i . The overall objective is to find an optimal joint policy $\pi = \langle \pi_1, \dots, \pi_n \rangle$ to maximize the joint value function $Q^\pi(s_t, \mathbf{u}_t) = \mathbb{E}[R_t | s_t, \mathbf{u}_t]$.

Value Decomposition. Value decomposition has emerged as a dominant paradigm in multi-agent reinforcement learning (MARL) under the centralized training and decentralized execution (CTDE) paradigm. It seeks to approximate the joint action-value function Q_{tot} by decomposing it into individual utility functions Q_i , where each utility depends solely on the agent’s local trajectory τ_i . To ensure that decentralized action selection remains consistent with the globally optimal joint action, the decomposition must satisfy the Individual-Global-Max (IGM) principle [11]:

$$\arg \max_{\mathbf{u}} Q_{tot}(\boldsymbol{\tau}, \mathbf{u}) = \{\arg \max_{u_1} Q_1(\tau_1, u_1), \dots, \arg \max_{u_n} Q_n(\tau_n, u_n)\}. \quad (1)$$

Among representative methods, VDN [21] implements a simple additive decomposition, treating all agents’ contributions equally by summing their utilities. To capture more complex coordination while preserving IGM, QMIX [11] introduces a mixing network that combines utilities into the joint value through a monotonic function. During training, the mixing network and agent networks are jointly optimized by minimizing the temporal-difference (TD) loss of Q_{tot} , while during execution, agents act independently using their local policies derived from the learned utility functions. The introduction of representative related works for the above formulation can be referred to in Appendix A.

3 High-order Interactions Modeling for Decomposition

In a large multi-agent task, agents are usually decomposed into several coalitions, each consisting of multiple agents that cooperate to accomplish the common goal. Besides, each agent could belong to different coalitions at different time steps. This coalition organization is general and can characterize most coordination patterns among agents. Thus, it is essential to model complex interactions among agents and estimate their credits for understanding their coordination patterns. In this section, we provide an informal comparative analysis of using the continued fraction network (CFN) architecture against widely adopted value decomposition methods: VDN [21], QMIX [11], and NA²Q [22].

From the view of value factorization, VDN provides a simple yet highly interpretable approach by representing the joint Q-value simply as the sum of individual agent Q-values, $Q_{tot}(\boldsymbol{\tau}, \mathbf{u}) =$

$\sum_{i \in N} Q_i(\tau_i, u_i)$. VDN inherently models only first-order interactions, which could limit its ability to capture richer and group-level coordination. QMIX enriches the functional class of factorisation than that of VDN by introducing a state-conditioned monotonic mixer $Q_{tot}(s, \tau, \mathbf{u}) = f_{\text{QMIX}}(s, [Q_1(\tau_1, u_1), \dots, Q_n(\tau_n, u_n)])$, where f_{QMIX} is constrained to be monotonic in each argument. This implicit higher-order modeling increases representational capacity, but at the expense of interpretability— f_{QMIX} behaves as a black box, obscuring which interactions drive performance. NA²Q tries to expand the joint value via a Taylor-like decomposition across all agents up to order n :

$$Q_{tot} = f_0 + \sum_{i=1}^n \alpha_i \underbrace{f_i(Q_i)}_{\text{order-1}} + \dots + \sum_{k \in \mathcal{D}_h} \alpha_k \underbrace{f_k(Q_k)}_{\text{order-}h} + \dots + \alpha_{1\dots n} \underbrace{f_{1\dots n}(Q_1, \dots, Q_n)}_{\text{order-}n}, \quad (2)$$

where $f_k \in \{f_1, \dots, f_{1\dots n}\}^m$ is modeled with neural additive model [23] and \mathcal{D}_h is the set of all non-empty subsets of $h \in \{1, \dots, n\}$ with order- h interactions. While this yields interpretability, low-order interaction terms (e.g., 2-order), the number of terms grows exponentially, $\mathcal{O}(2^n)$, making full expansion impractical for large teams.

To overcome the limitations of existing value decomposition methods discussed above, we enrich with the value factorization via a continued fraction neural network (CFN) inspired by CoFrNets [18], whose recursive structure and linear composition form a function class with universal approximation capability [24]. Following the terminology of CoFrNets, we call the function depicted in Fig. 1 a “ladder”, as its pictorial representation resembles a rail-and-rung structure that sequentially propagates inputs through the nodes. The joint action-value function can be established as a weighted summation of individual values:

$$Q_{tot} = \sum_{k=1}^l \alpha_k \cdot \tilde{f}_k(\mathbf{Q}), \quad (3)$$

where \tilde{f}_k denotes a continued fraction structure $\frac{1}{w_{k_1}Q + \frac{1}{w_{k_2}Q + \dots}}$ with linear functions w_k of the input $\mathbf{Q} = \{Q_1, \dots, Q_n\}$ given l ladders, and α_k are learnable weights used to estimate the contribution of individual agents and coalitions of agents. With a power series expansion, such a recursive structure can be rewritten as

$$\frac{1}{w_1Q + \frac{1}{w_2Q + \dots}} = \sum_{p_1, \dots, p_n=0}^{\infty} c_{p_1, \dots, p_n} \prod_{i=1}^n Q_i^{p_i}, \quad (4)$$

where the coefficients c_{p_1, \dots, p_n} and the weight parameters w_k are in one-to-one correspondence [17, 18], and each c_{p_1, \dots, p_n} used to derive interactions among agents.

CFN generally approximates interactions up to a finite depth d , which constitutes a rational approximation $R_d(\mathbf{Q})$ of the joint utility function up to d -order interactions among agents. It shows that truncating the continued fraction provides a practical rational approximation that explicitly models agent interactions up to order d :

$$\hat{Q}_k = \frac{1}{w_1Q + \frac{1}{w_2Q + \dots}} \frac{1}{w_dQ} = \sum_{p_1, \dots, p_n=0}^d c_{p_1, \dots, p_n} \prod_{i=1}^n Q_i^{p_i}. \quad (5)$$

Definition 1 (Padé Approximant [25, 26]). *Let $C(z) = \sum_{k=0}^{\infty} c_k z^k$ be a formal power series in the variable z , then the Padé approximant of order $[L/M]$ is a rational function of the form:*

$$R_{L,M}(z) = [A_{L,M}(z)]/[B_{L,M}(z)], \quad (6)$$

where $A_{L,M}(z)$ and $B_{L,M}(z)$ are polynomials of degrees at most L and M , respectively, chosen such that

$$B_{L,M}(z)C(z) - A_{L,M}(z) = \mathcal{O}(z^{L+M+1}), \quad (7)$$

where notation $\mathcal{O}(z^k)$ denotes some power series of the form $\sum_{n=k}^{\infty} \tilde{c}_n z^n$. This approximation minimizes the difference between the rational function and the power series up to the order $L + M$.

We give a formal proof that such truncation naturally satisfies the Padé approximation condition as defined in Definition 1, i.e., $f(\mathbf{Q}) - R_d(\mathbf{Q}) = \mathcal{O}(Q^{d+1})$, where $f(\mathbf{Q})$ denotes the complete representation of agent interactions based on their individual value functions. This implies that the

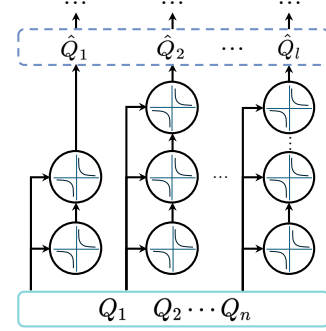


Figure 1: A diagram of CFN composed of different depth ladders that take individual values \mathbf{Q} as inputs and output temporal values \hat{Q} with d -order interactions.

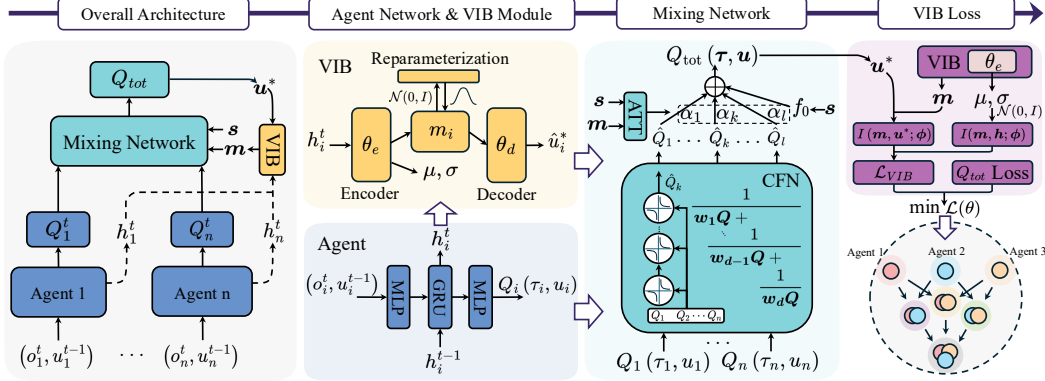


Figure 2: The overall architecture of QCoFr. A CFN-based mixing network models high-order interactions among agents by expressing Q_{tot} as a linear combination of l ladders over individual values Q . The VIB module encodes the hidden state h into assistive information m , which is used to deduce the credits of each agent of coalitions together with the global state s .

depth- d truncation of the continued fraction yields an exact approximation of $f(Q)$ up to the d -th order of Q . The detailed proof is provided in Appendix B.2.

Moreover, we can easily control the capacity of the interaction order among agents with the acceptable complexity $\mathcal{O}(n)$ by adjusting the depth of CFN. Since linear combinations of CF modules constitute a function class with universal approximation power [24], they can approximate any continuous mapping between finite-dimensional spaces. Its recursive and interpretable structure reveals the contributions of individual agents and coalitions of agents, enabling precise credit assignment while faithfully modeling high-order interactions among agents. We also study two CFN variants, CFN-C and CFN-D (see Fig. 10 and Appendix C.6). CFN-C combines single-feature and full-input CF ladders, trading higher expressivity for additional computational cost. CFN-D retains only single-feature ladders, yielding a purely additive mixer that cannot represent higher-order interactions. Empirical comparisons are provided in Section 5.2.

4 Methods

We next present an interpretable value decomposition framework that explicitly models arbitrary-order agent interactions without incurring a combinatorial explosion. The overall architecture of QCoFr is illustrated in Fig. 2, which consists of three components as follows: (1) an individual action-value function for each agent, (2) an assistive information generation module that encodes the hidden state h via a variational information bottleneck (VIB) [19] to produce the assistive information m to promote the credit assignment, and (3) a joint action-value function Q_{tot} that composes individual action-value functions into a joint action-value function using a CFN architecture, where the assistive information m and the global state s are fed into the mixing network to estimate credits. During the centralized training, the whole network is learned in an end-to-end fashion to minimize the sum of TD and VIB loss, and each agent selects actions using its Q-function based on local action-observation history in a decentralized fashion.

Individual Action-value Function is computed by a recurrent Q-network with gated recurrent unit (GRU) for each agent i , which takes the local observation o_i^t , historical information h_i^{t-1} , and previous action u_i^{t-1} as inputs and outputs local $Q_i(\tau_i, u_i)$.

Assistive Information Generation Module. Previous works usually use all available information for estimating the credit assignment α_k , which could be quite inefficient [27]. The global state s is an unobserved confounder as the common cause factor of the global state and the joint value function [28, 22]. Thus, it will be necessary to introduce additive information to cut off the confounder. To this end, we generate an assistive latent representation m from the hidden state h of agents to predict the optimal action selection u^* , which forms the Markov dependency $h \rightarrow m \rightarrow u^*$. Here, we utilize VIB to capture the task-relevant information that can provide a more accurate estimation of the optimal joint action selection from the hidden state h , which can promote the credit assignment. The goal is to learn an encoding that contains as little redundant information as possible while

providing maximal information about the prediction \mathbf{u}^* that affects environmental information or its private properties, which can be written as

$$J_{IB}(\phi) = I(\mathbf{m}, \mathbf{u}^*; \phi) - \beta I(\mathbf{m}, \mathbf{h}; \phi), \quad (8)$$

where the Lagrange multiplier $\beta \geq 0$ controls the tradeoff. Here, we adopt variational approximations to simplify the computation of the mutual information I in Eq. 8. The following theorems provide tractable bounds for each term.

Theorem 1 (Lower Bound for $I(\mathbf{m}, \mathbf{u}^*; \phi)$). *Let the representation m_i be reparameterized as a random variable drawn from a multivariate Gaussian distribution $m_i \sim \mathcal{N}(f_m(h_i; \phi_m), \mathbf{I})$, where f_m is an encoder parameterized by ϕ_m , h_i denotes the hidden state of agent i , and \mathbf{I} is the identity covariance matrix. Then, the mutual information between the assistive information \mathbf{m} and the optimal joint action \mathbf{u}^* is lower-bounded as:*

$$I(\mathbf{m}, \mathbf{u}^*; \phi) \geq \frac{1}{N} \sum_{i=1}^N \mathbb{E}_{\epsilon \sim p(\epsilon)} [-\log q(u_i^* | f(h_i, \epsilon))], \quad (9)$$

where $q(u_i^* | m_i)$ is a variational distribution approximating the true posterior $p(u_i^* | m_i)$, and $m_i = f(h_i, \epsilon)$ denotes a deterministic function of h_i and the Gaussian random variable ϵ .

Proof sketch: This bound follows from the variational representation of mutual information. By introducing a variational approximation $q(u_i^* | m_i)$ and applying the reparameterization trick [29] to write $p(m_i | h_i) dm_i = p(\epsilon) d\epsilon$, the intractable posterior is replaced with a more manageable form, enabling efficient optimization via gradient-based methods.

Theorem 2 (Upper Bound for $I(\mathbf{m}, \mathbf{h}; \phi)$). *Let $\tilde{q}(\mathbf{m})$ denote a variational approximation of the marginal distribution $p(\mathbf{m})$. Then, the mutual information between the representation \mathbf{m} and the hidden state \mathbf{h} admits the following upper bound:*

$$I(\mathbf{m}, \mathbf{h}; \phi) \leq \text{KL}(p(\mathbf{m} | h_i) \| \tilde{q}(\mathbf{m})). \quad (10)$$

Proof sketch: This result exploits the non-negativity of the KL divergence. By approximating the marginal distribution $p(\mathbf{m})$ with a variational approximation $\tilde{q}(\mathbf{m})$, the mutual information can be bounded from above via the definition of the KL divergence.

Combining the above conclusions, we can arrive at the following variational objective function:

$$\mathcal{L}_{VIB} = \frac{1}{N} \sum_{i=1}^N \mathbb{E}_{\epsilon \sim p(\epsilon)} [-\log q(u_i^* | f(h_i, \epsilon))] + \beta \text{KL}[p(\mathbf{m} | h_i), \tilde{q}(\mathbf{m})]. \quad (11)$$

The detailed derivation and rigorous proofs for these bounds are provided in Appendix B.1.

Mixing Network. We introduce the CFN-based mixing network consisting of l ladders (Fig. 2) with a maximum depth d , which are designed to model d -order interactions among agents. Each ladder k takes the local value functions \mathbf{Q} as input and produces an output \hat{Q}_k as defined in Eq. 5. To satisfy the IGM principle [30], each CFN layer adopts a strictly non-negative activation function of the form $\frac{1}{\max(|z|, \delta)}$, where z denotes the sum of the current weighted input and the reciprocal of the previous layer’s output, and δ is a small positive constant to prevent poles caused by near-zero denominators. Since the universal approximation theorem applies to any linear combination of continued fractions and does not rely on non-negative weights, an extension to non-IGM mixers is possible, with details discussed in the Appendix E.2.

Effective coordination hinges on precisely deducing the contributions of each individual agent or coalition to the overall success. To this end, we leverage assistive information \mathbf{m} together with the global state \mathbf{s} to estimate the credits. Specifically, the credit α_k for each ladder k is computed as

$$\alpha_k = \frac{\exp\left((\mathbf{w}_m \mathbf{m})^\top \text{ReLU}(\mathbf{w}_s \mathbf{s})\right)}{\sum_{k=1}^l \exp\left((\mathbf{w}_m \mathbf{m})^\top \text{ReLU}(\mathbf{w}_s \mathbf{s})\right)}, \quad (12)$$

where the weights \mathbf{w}_m and \mathbf{w}_s are the learnable parameters, and ReLU is the activation function. When the credits α_k are then used to aggregate the outputs \hat{Q}_k of the ladders, the joint action-value function Q_{tot} can be represented as

$$Q_{tot} = \sum_{k=1}^l \alpha_k \hat{Q}_k = \sum_{k=1}^l \alpha_k \sum_{p_1, \dots, p_n=0}^d c_{p_1, \dots, p_n} \prod_{i=1}^n Q_i^{p_i} = \sum_{p_1, \dots, p_n=0}^d c'_{p_1, \dots, p_n} \prod_{i=1}^n Q_i^{p_i}, \quad (13)$$

where c'_{p_1, \dots, p_n} denotes the final coefficient of each interaction term. For notational simplicity when discussing interaction patterns, we denote the coefficient of a specific agent interaction (e.g., agent i and j) as β_{ij} , where the subscript indicates the agent indices involved.

Overall Learning Objective. To sum up, we train QCoFr end-to-end with two terms of loss functions. The first one is naturally the original mean-squared temporal-difference (TD) error, which enables each agent to learn its individual agent policy by optimizing the joint-action value of the mixing network module. The last one is the VIB loss \mathcal{L}_{VIB} that is encouraged to produce assistive information. Thus, the overall loss function is formulated as follows:

$$\mathcal{L}(\theta) = \sum_i (Q_{tot}(s, \tau, \mathbf{u}) - y_i)^2 + \mathcal{L}_{VIB}, \quad (14)$$

where $y_i = r + \gamma \hat{Q}_{tot}(s', \tau', \arg \max_{\mathbf{u}' \in \mathcal{U}^n} Q_{tot}(s', \tau', \mathbf{u}'))$ with θ denotes the parameters of the target network. We summarize the full pseudo-code of QCoFr in Appendix C.1.

5 Experiments

In this section, we conduct experiments to evaluate QCoFr on three challenging benchmarks over the Level Based foraging (LBF) [31], the StarCraft Multi-Agent Challenge (SMAC) [32] and SMACv2 [33]. The details of the environment can be found in Appendix C. We compare our method against nine prominent baselines, including VDN [21], QMIX [11], QPLEX [34], Centrally-Weighted QMIX (CW-QMIX) [35], CDS [36], SHAQ [37], GoMARL [38], ReBorn [39], and NA²Q [22]. We carry out experiments with 5 random seeds, and all performance results are plotted using mean \pm std. Furthermore, we perform interpretability analyses of QCoFr to provide empirical evidence for the contributions of individual agents and coalitions of agents.

5.1 Performance Comparison

Performance on LBF. We first evaluate QCoFr on two constructed LBF tasks: 3 agents with 3 food items (*lbf-3-3*) and 4 agents with 2 food items (*lbf-4-2*). LBF is a grid-based multi-agent benchmark that supports configurable levels of cooperation and observability [40]. Each agent navigates a 10×10 grid world and observes a 2×2 sub-grid centered around it, where a group of adjacent agents can successfully collect a food item if

the sum of their levels is greater than or equal to the item’s level. As shown in Fig. 3, QCoFr achieves competitive performance compared to state-of-the-art methods. However, the simplified task design inherently constrains the model’s capacity to fully leverage higher-order interaction mechanisms, whose potential advantages may emerge in complex multi-agent coordination scenarios. The failure of the CDS may be due to an overemphasis on behavioral diversity without considering effective coordination among agents. QMIX has a slow convergence speed due to its inability to exploit latent information, which restricts its representational capacity. GoMARL and ReBorn also require more steps to discover effective agent groupings and allocate neuron weights. While CW-QMIX, NA²Q, and SHAQ demonstrate competitive performance by introducing additional modules to enhance value decomposition, their inability to model higher-order interactions or reliance on complex computation may hinder scalability in complex multi-agent coordination tasks.

Performance on SMAC. We next compare QCoFr with baselines on the more challenging SMAC benchmark, where agents make decisions based on local observations while cooperating to defeat AI-controlled enemies. We show the performance comparison on six different scenarios, including one easy map: *2s3z*, three hard maps: *2c_vs_64zg*, *3s_vs_5z*, *5m_vs_6m*, and two super-hard maps: *3s5z_vs_3s6z*, *6h_vs_8z*. As shown in Fig. 4, QCoFr achieves superior performance across almost all

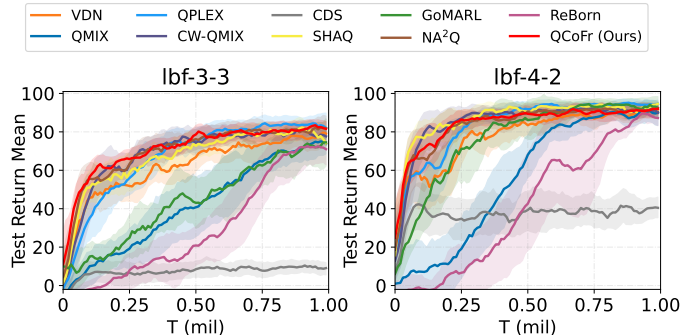


Figure 3: Performance results on LBF benchmark.

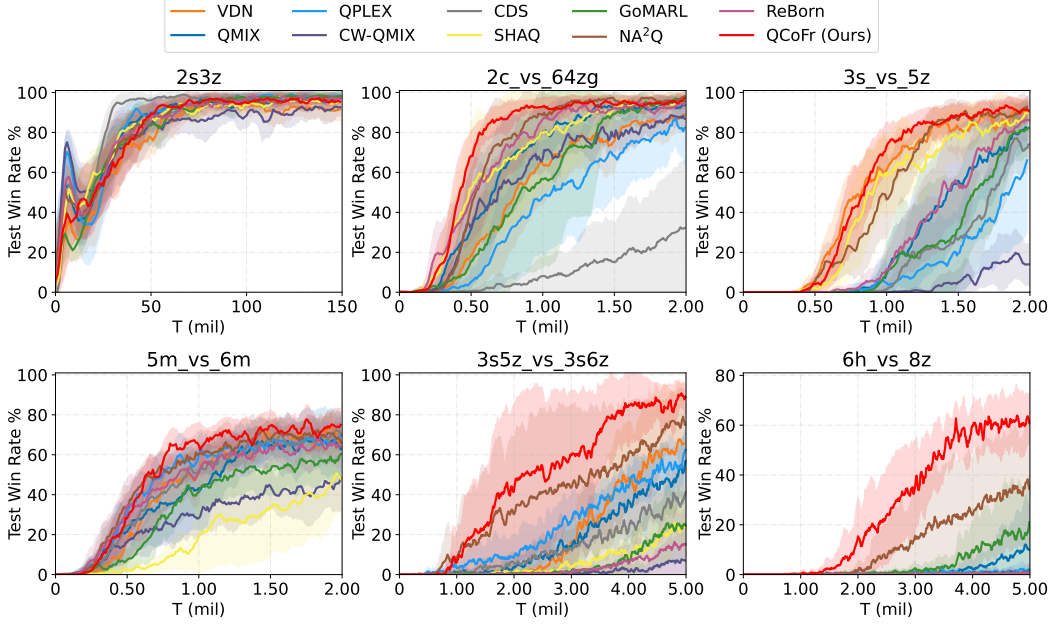


Figure 4: Performance results on SMAC benchmark.

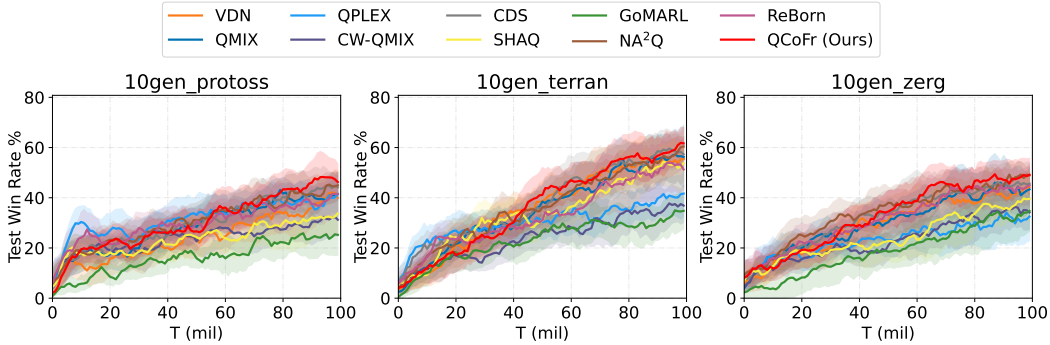


Figure 5: Performance results on SMACv2 benchmark.

scenarios, especially on the super hard tasks. CW-QMIX and QPLEX do not achieve satisfactory performance, which may be due to excessive approximation and the relaxed constraints introduced during training. CDS exhibits slower convergence rates, which may be due to requiring more training steps to capture diverse individualized behaviors. Although GoMARL and NA²Q can model high-order interactions to yield notable performance on complex scenarios by leveraging grouping and enumeration, GoMARL requires extended training durations to learn effective groupings, and NA²Q considers low-order interaction terms to avoid combinatorial explosion.

Performance on SMACv2. We evaluate QCoFr performance on three scenarios from SMACv2, including *zerg_5_vs_5*, *protoss_5_vs_5*, and *terran_5_vs_5*. SMACv2 introduces randomly generated and positioned for unit, increasing environmental stochasticity compared to SMAC. The performance of QCoFr is significantly better than other algorithms across all scenarios. In contrast, GoMARL performs the worst, which is due to its dynamic grouping structure, leading to slow convergence. While SHAQ demonstrates marginally superior performance, its inability to model higher-order agent interactions limits its adaptability to all maps. Compared to NA²Q, QMIX, and CDS, QCoFr achieves better performance, which should benefit from the assistive information for estimating credit assignment, especially for the high-order interaction patterns among agents.

5.2 Ablation Studies

To discuss the influence of each component, we conduct ablation studies about (a) the number of interaction orders among agents, (b) the CFN structure, and assistive information on performance.

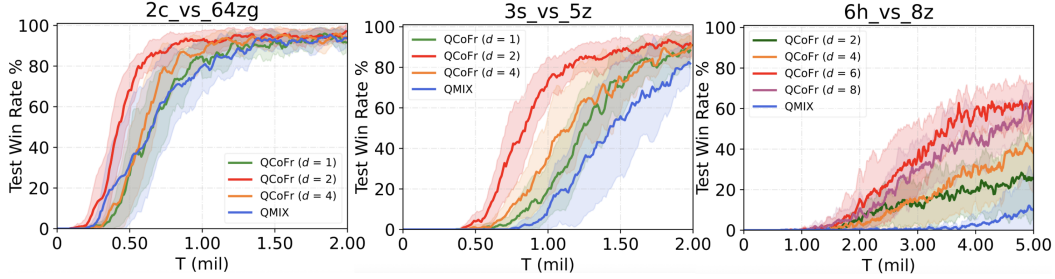


Figure 6: Comparison of different numbers of interaction orders.

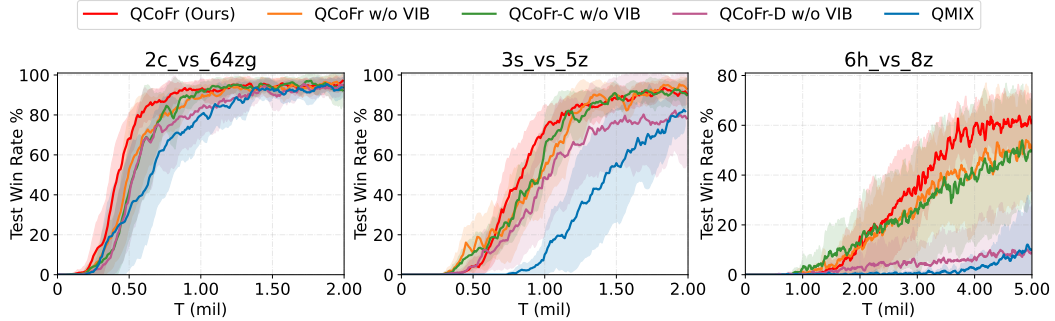


Figure 7: Performance with and without VIB and comparison of different CFN structures.

The Number of Interaction Orders. We conduct ablation experiments by varying the depth d of CFN, which governs the highest order of inter-agent interactions modeled by the framework. On $2c_vs_64zg$ and $3s_vs_5z$ maps, $QCoFr (d = 2)$ yields significant performance improvements compared to $QCoFr (d = 1)$, which underscores the importance of explicitly modeling higher-order inter-agent effects as shown in *Fig. 6*. However, beyond the optimum, performance could degrade, likely due to overfitting to spurious higher-order correlations. The same trend emerges in the $6h_vs_8z$ scenario, where the model achieves its best performance with depth $d = 6$ before degrading with further depth increases. These findings demonstrate that modeling higher-order interactions yields performance improvements for complex coordination tasks, but only within a bounded regime that aligns with the task’s intrinsic interaction complexity. Notably, our method using a single-layer CFN still outperforms QMIX, which confirms that the assistive information can better help deduce the contribution of agents for their team.

Impact of CFN Structure and Assistive Information Module. To validate the effectiveness of the CFN structure, we compare $QCoFr w/o VIB$ against two CFN-based variants— $QCoFr-C w/o VIB$ and $QCoFr-D w/o VIB$, under a unified setting without the VIB module. As shown in *Fig. 7*, $QCoFr w/o VIB$ achieves comparable performance to $QCoFr-C w/o VIB$, while offering a simpler structure and lower computational cost. In contrast, $QCoFr-D w/o VIB$ exhibits significantly degraded performance, especially on the $6h_vs_8z$ scenario, which underscores the necessity of explicit inter-agent interaction modeling for complex tasks. To summarize, we adopt CFN as the backbone for its ability to capture higher-order interactions with a simple, efficient design. By integrating a VIB-based assistive information generation module, QCoFr achieves significant improvements in both convergence speed and final performance, demonstrating its efficacy and practical utility. More additional ablations in Appendix E.1 detail the respective contributions of the VIB and CFN modules.

5.3 Interpretability

To intuitively demonstrate the interpretability of QCoFr, we demonstrate $QCoFr (d = 2)$ and $QCoFr (d = 4)$ and display some key frames on $5m_vs_6m$ scenario. As shown in *Fig. 8(b)*, the pairwise coalitions (agent 3, agent 4) and (agent 3, agent 5) emerge as coordinated coalitions that focus fire on the same enemy unit. Here, we find that they have higher coalition contributions of 3.884 and 3.339 than the others. In contrast, agent 1 disengages from combat when it has low health value to avoid early elimination, which indicates that it does not contribute to the team and obtains a lower contribution of 0.552. These observations highlight QCoFr’s ability to facilitate diverse role

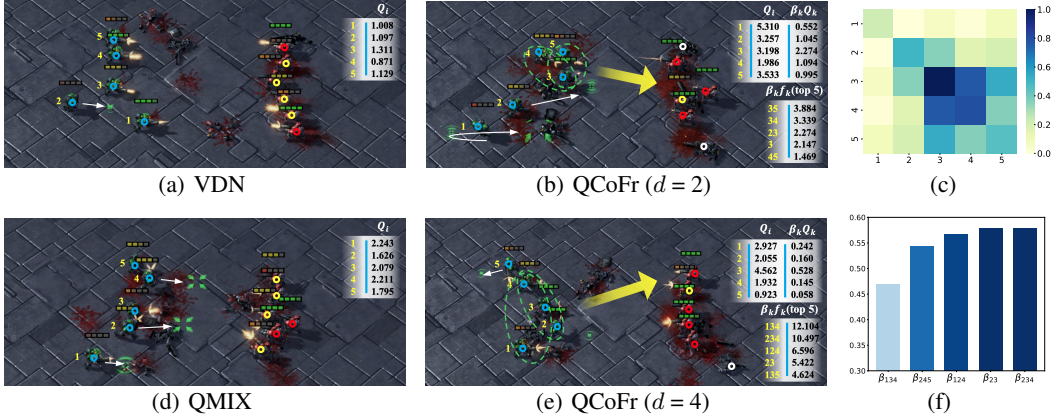


Figure 8: Visualization of evaluation results for QCoFr and baselines on *5m_vs_6m* map. (b) and (e) illustrate the behaviors of QCoFr with CFN depths of 2 and 4 at a specific time step. (c) visualizes the weights of individual agents and pairwise coalitions corresponding to the behavior shown in (b), while (f) presents the top five highest-weighted coalitions extracted from (e), due to the increased number of possible interactions. (a) and (d) show the behaviors of VDN and QMIX for comparison.

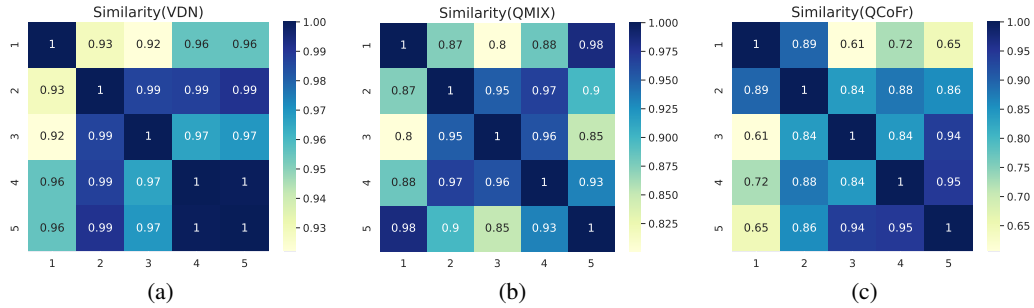


Figure 9: Visualization of agent diversity via QCoFr and baselines. Cosine similarities of agent Q-values under the same observation indicate that QCoFr yields more diverse agent behaviors.

specializations and demonstrate the advantage of modeling agent interactions, which helps deduce the contribution of individual agents and coalitions within their team.

Further, we show the behavior of the agents when $d = 4$ for QCoFr to demonstrate that the model captures complex agent cooperation as shown in *Fig. 8(e)*. As shown in *Fig. 8(c)*, the weights are predominantly concentrated on agent 3 and agent 4, as well as their interactions with other agents, consistent with their coordinated attacks. While in deeper QCoFr, top-ranked terms are predominantly higher-order, such as interactions among agents 1, 3, and 4, which yield the highest contributions, demonstrating the model’s capacity to encode intricate cooperative dynamics. In contrast, QMIX and VDN produce less differentiated policies, with individual Q-values remaining close, making their decision logic harder to interpret. Furthermore, as shown in *Fig. 8(a)* and *Fig. 8(d)*, agents under VDN and QMIX frequently attack multiple enemy units simultaneously, leading to prolonged numerical disadvantage and increased failure risk.

To evaluate whether QCoFr facilitates more diverse agent behaviors during training, we compute the cosine similarity of individual Q-values under the same observation across different methods, as shown in *Fig. 9*. QCoFr yields consistently lower similarity, which indicates more diverse and thus more specialized agent preferences, in line with the qualitative findings in *Fig. 8*. In contrast, VDN and QMIX maintain similarity close to 1, which reflects homogenized preferences that hinder the emergence of complex cooperative strategies and obscure individual decision-making.

6 Conclusion

In this paper, we introduce QCoFr, an interpretable value-based MARL framework grounded in the expressive and compact structure of continued fractions. By leveraging continued fraction neural networks and a variational information bottleneck over agent histories, QCoFr explicitly models agent

interactions of arbitrary order while maintaining low model complexity and inherent interpretability. Extensive experiments show that QCoFr matches or surpasses strong value-decomposition baselines and yields clearer attributions to individuals and coalitions. We believe QCoFr presents a promising direction for designing MARL algorithms with mathematically grounded, interpretable structures and highlights the importance of modeling higher-order coordination. Future work will explore adaptive mechanisms to dynamically adjust the depth of interaction modeling in response to task complexity.

Limitations. In the current implementation, the CFN depth is fixed per task, which may be suboptimal or wasteful. A promising direction is to adapt depth during training (or per state) to balance computation with representational power.

7 Acknowledgements

This work was supported in part by the China Postdoctoral Science Foundation under Grant Number 2025T180877, the Jiangsu Funding Program for Excellent Postdoctoral Talent 2025ZB267, the National Key Research and Development Program of China under Grant 2023YFD2001003, Major Science and Technology Project of Jiangsu Province under Grant BG2024041, and the Fundamental Research Funds for the Central Universities under Grant 011814380048.

References

- [1] Afshin Oroojlooy and Davood Hajinezhad. A review of cooperative multi-agent deep reinforcement learning. *Applied Intelligence*, 53(11):13677–13722, 2023.
- [2] Songyang Han, He Wang, Sanbao Su, Yuanyuan Shi, and Fei Miao. Stable and efficient Shapley value-based reward reallocation for multi-agent reinforcement learning of autonomous vehicles. In *International Conference on Robotics and Automation*, pages 8765–8771, 2022.
- [3] Zhili Zhang, Songyang Han, Jiangwei Wang, and Fei Miao. Spatial-temporal-aware safe multi-agent reinforcement learning of connected autonomous vehicles in challenging scenarios. In *International Conference on Robotics and Automation*, pages 5574–5580, 2023.
- [4] Joris Dinneweth, Abderrahmane Boubezoul, René Mandiau, and Stéphane Espié. Multi-agent reinforcement learning for autonomous vehicles: A survey. *Autonomous Intelligent Systems*, 2(1):27, 2022.
- [5] Yixin Huang, Shufan Wu, Zhongcheng Mu, Xiangyu Long, Sunhao Chu, and Guohong Zhao. A multi-agent reinforcement learning method for swarm robots in space collaborative exploration. In *International Conference on Control, Automation and Robotics*, pages 139–144, 2020.
- [6] Weizheng Wang, Le Mao, Ruiqi Wang, and Byung-Cheol Min. Multi-robot cooperative socially-aware navigation using multi-agent reinforcement learning. In *International Conference on Robotics and Automation*, pages 12353–12360, 2024.
- [7] Tong Zhou, Dunbing Tang, Haihua Zhu, and Zequn Zhang. Multi-agent reinforcement learning for online scheduling in smart factories. *Robotics and Computer-Integrated Manufacturing*, 72:102202, 2021.
- [8] Aleksandar Krnjaic, Raul D Steleac, Jonathan D Thomas, Georgios Papoudakis, Lukas Schäfer, Andrew Wing Keung To, Kuan-Ho Lao, Murat Cubuktepe, Matthew Haley, Peter Börsting, et al. Scalable multi-agent reinforcement learning for warehouse logistics with robotic and human co-workers. In *International Conference on Intelligent Robots and Systems*, pages 677–684, 2024.
- [9] Yaodong Yang, Rui Luo, Minne Li, Ming Zhou, Weinan Zhang, and Jun Wang. Mean field multi-agent reinforcement learning. In *International Conference on Machine Learning*, pages 5571–5580, 2018.
- [10] Daan Bloembergen, Karl Tuyls, Daniel Hennes, and Michael Kaisers. Evolutionary dynamics of multi-agent learning: A survey. *Journal of Artificial Intelligence Research*, 53:659–697, 2015.

- [11] Tabish Rashid, Mikayel Samvelyan, Christian Schroeder, Gregory Farquhar, Jakob Foerster, and Shimon Whiteson. QMIX: Monotonic value function factorisation for deep multi-agent reinforcement learning. In *International Conference on Machine Learning*, pages 4295–4304, 2018.
- [12] Jianhong Wang, Yuan Zhang, Tae-Kyun Kim, and Yunjie Gu. Shapley Q-value: A local reward approach to solve global reward games. In *AAAI Conference on Artificial Intelligence*, pages 7285–7292, 2020.
- [13] Tsuyoshi Goto, Hidenori Itaya, Tsubasa Hirakawa, Takayoshi Yamashita, and Hironobu Fujiyoshi. Solving the deadlock problem with deep reinforcement learning using information from multiple vehicles. In *2022 IEEE Intelligent Vehicles Symposium*, pages 1026–1032, 2022.
- [14] Stephanie Milani, Zhicheng Zhang, Nicholay Topin, Zheyuan Ryan Shi, Charles Kamhoua, Evangelos E Papalexakis, and Fei Fang. MAVIPER: Learning decision tree policies for interpretable multi-agent reinforcement learning. In *Joint European Conference on Machine Learning and Knowledge Discovery in Databases*, pages 251–266, 2022.
- [15] Zichuan Liu, Yuanyang Zhu, Zhi Wang, Yang Gao, and Chunlin Chen. MIXRTs: Toward interpretable multi-agent reinforcement learning via mixing recurrent soft decision trees. *IEEE Transactions on Pattern Analysis and Machine Intelligence*, 47(5):4090–4107, 2025.
- [16] Daniël Vos and Sicco Verwer. Optimizing interpretable decision tree policies for reinforcement learning. *arXiv preprint arXiv:2408.11632*, 2024.
- [17] Carl M Bender and Kimball A Milton. Continued fraction as a discrete nonlinear transform. *Journal of Mathematical Physics*, 35(1):364–367, 1994.
- [18] Isha Puri, Amit Dhurandhar, Tejaswini Pedapati, Karthikeyan Shanmugam, Dennis Wei, and Kush R Varshney. CoFrNets: interpretable neural architecture inspired by continued fractions. In *Advances in Neural Information Processing Systems*, pages 21668–21680, 2021.
- [19] Alexander A Alemi, Ian Fischer, Joshua V Dillon, and Kevin Murphy. Deep variational information bottleneck. In *International Conference on Learning Representations*, 2017.
- [20] Frans A Oliehoek and Christopher Amato. *A concise introduction to decentralized POMDPs*, volume 1. Springer, 2016.
- [21] Peter Sunehag, Guy Lever, Audrunas Gruslys, Wojciech Marian Czarnecki, Vinicius Zambaldi, Max Jaderberg, Marc Lanctot, Nicolas Sonnerat, Joel Z Leibo, Karl Tuyls, et al. Value-decomposition networks for cooperative multi-agent learning based on team reward. In *International Conference on Autonomous Agents and Multi-Agent Systems*, pages 2085–2087, 2018.
- [22] Zichuan Liu, Yuanyang Zhu, and Chunlin Chen. NA²Q: Neural attention additive model for interpretable multi-agent Q-learning. In *International Conference on Machine Learning*, pages 22539–22558, 2023.
- [23] Rishabh Agarwal, Levi Melnick, Nicholas Frosst, Xuezhou Zhang, Ben Lengerich, Rich Caruana, and Geoffrey E Hinton. Neural additive models: Interpretable machine learning with neural nets. In *Advances in Neural Information Processing Systems*, pages 4699–4711, 2021.
- [24] Kurt Hornik, Maxwell Stinchcombe, and Halbert White. Multilayer feedforward networks are universal approximators. *Neural Networks*, 2(5):359–366, 1989.
- [25] George A Baker Jr and John L Gammel. The padé approximant. *Journal of Mathematical Analysis and Applications*, 2(1):21–30, 1961.
- [26] Lisa Lorentzen. Padé approximation and continued fractions. *Applied Numerical Mathematics*, 60(12):1364–1370, 2010.
- [27] Weixun Wang, Tianpei Yang, Yong Liu, Jianye Hao, Xiaotian Hao, Yujing Hu, Yingfeng Chen, Changjie Fan, and Yang Gao. Action semantics network: Considering the effects of actions in multiagent systems. In *International Conference on Learning Representations*, 2020.

- [28] Jiahui Li, Kun Kuang, Baoxiang Wang, Furui Liu, Long Chen, Changjie Fan, Fei Wu, and Jun Xiao. Deconfounded value decomposition for multi-agent reinforcement learning. In *International Conference on Machine Learning*, pages 12843–12856, 2022.
- [29] Diederik P Kingma and Max Welling. Auto-encoding variational Bayes. In *International Conference on Learning Representations*, 2014.
- [30] Kyunghwan Son, Daewoo Kim, Wan Ju Kang, David Earl Hostallero, and Yung Yi. QTRAN: Learning to factorize with transformation for cooperative multi-agent reinforcement learning. In *International Conference on Machine Learning*, pages 5887–5896, 2019.
- [31] Filippos Christianos, Lukas Schäfer, and Stefano V Albrecht. Shared experience actor-critic for multi-agent reinforcement learning. In *Advances in Neural Information Processing Systems*, pages 10707–10717, 2020.
- [32] Mikayel Samvelyan, Tabish Rashid, Christian Schroeder De Witt, Gregory Farquhar, Nantas Nardelli, Tim GJ Rudner, Chia-Man Hung, Philip HS Torr, Jakob Foerster, and Shimon Whiteson. The StarCraft multi-agent challenge. In *International Joint Conference on Autonomous Agents and Multi-Agent Systems*, 2019.
- [33] Benjamin Ellis, Jonathan Cook, Skander Moalla, Mikayel Samvelyan, Mingfei Sun, Anuj Mahajan, Jakob Foerster, and Shimon Whiteson. SMACv2: An improved benchmark for cooperative multi-agent reinforcement learning. In *Advances in Neural Information Processing Systems*, pages 37567–37593, 2023.
- [34] Jianhao Wang, Zhizhou Ren, Terry Liu, Yang Yu, and Chongjie Zhang. QPLEX: Duplex dueling multi-agent Q-learning. In *International Conference on Learning Representations*, 2020.
- [35] Tabish Rashid, Gregory Farquhar, Bei Peng, and Shimon Whiteson. Weighted QMIX: Expanding monotonic value function factorisation for deep multi-agent reinforcement learning. In *Advances in Neural Information Processing Systems*, pages 10199–10210, 2020.
- [36] Chenghao Li, Tonghan Wang, Chengjie Wu, Qianchuan Zhao, Jun Yang, and Chongjie Zhang. Celebrating diversity in shared multi-agent reinforcement learning. In *Advances in Neural Information Processing Systems*, pages 3991–4002, 2021.
- [37] Jianhong Wang, Yuan Zhang, Yunjie Gu, and Tae-Kyun Kim. SHAQ: Incorporating Shapley value theory into multi-agent Q-learning. In *Advances in Neural Information Processing Systems*, pages 5941–5954, 2022.
- [38] Yifan Zang, Jinmin He, Kai Li, Haobo Fu, Qiang Fu, Junliang Xing, and Jian Cheng. Automatic grouping for efficient cooperative multi-agent reinforcement learning. In *Advances in Neural Information Processing Systems*, pages 46105–46121, 2023.
- [39] Haoyuan Qin, Chennan Ma, Deng Deng, Zhengzhu Liu, Songzhu Mei, Xinwang Liu, Cheng Wang, and Siqi Shen. The dormant neuron phenomenon in multi-agent reinforcement learning value factorization. In *Advances in Neural Information Processing Systems*, pages 35727–35759, 2024.
- [40] Georgios Papoudakis, Filippos Christianos, Lukas Schäfer, and Stefano V. Albrecht. Benchmarking multi-agent deep reinforcement learning algorithms in cooperative tasks. In *Neural Information Processing Systems Track on Datasets and Benchmarks*, 2021.
- [41] Frans A Oliehoek, Matthijs TJ Spaan, and Nikos Vlassis. Optimal and approximate Q-value functions for decentralized pomdps. *Journal of Artificial Intelligence Research*, 32:289–353, 2008.
- [42] Landon Kraemer and Bikramjit Banerjee. Multi-agent reinforcement learning as a rehearsal for decentralized planning. *Neurocomputing*, 190:82–94, 2016.
- [43] Sarit Kraus, Amos Azaria, Jelena Fiosina, Maike Greve, Noam Hazon, Lutz Kolbe, Tim-Benjamin Lembecke, Jorg P Muller, Soren Schleibaum, and Mark Vollrath. AI for explaining decisions in multi-agent environments. In *AAAI Conference on Artificial Intelligence*, pages 13534–13538, 2020.

- [44] Shariq Iqbal and Fei Sha. Actor-attention-critic for multi-agent reinforcement learning. In *International Conference on Machine Learning*, pages 2961–2970, 2019.
- [45] Jiachen Yang, Igor Borovikov, and Hongyuan Zha. Hierarchical cooperative multi-agent reinforcement learning with skill discovery. In *International Conference on Autonomous Agents and Multi-Agent Systems*, 2020.
- [46] Lingxiang Yun, Di Wang, and Lin Li. Explainable multi-agent deep reinforcement learning for real-time demand response towards sustainable manufacturing. *Applied Energy*, 347:121324, 2023.
- [47] Trevor Hastie and Robert Tibshirani. *Generalized additive models*, volume 43. CRC Press, 1990.
- [48] Zhiwei Xu, Bin Zhang, Guangchong Zhou, Zeren Zhang, Guoliang Fan, et al. Dual self-awareness value decomposition framework without individual global max for cooperative MARL. In *Advances in Neural Information Processing Systems*, pages 73898–73918, 2023.

A Related Work

Value Decomposition. Centralized training with decentralized execution (CTDE) has emerged as a powerful paradigm in MARL [41, 42], where global information can be accessed during centralized training and learned policies are executed with only local information in a decentralized way. Under the CTDE paradigm, value decomposition methods show their strength in expressing the joint value function conditioned on individual value functions. VDN [21] introduces a linear decomposition, representing the joint Q-value as a sum of agent-wise Q-values. However, its additive nature ignores inter-agent interactions, limiting its scalability to complex coordination tasks. QMIX [11] improves representational capacity by employing a nonlinear monotonic mixing network parameterized via hypernetworks, but the imposed monotonicity constraint hinders its flexibility. To overcome this, QTRAN [30] introduces a relaxed transformation-based decomposition to bypass monotonicity, while WQMIX [35] incorporates a weighted projection to enhance approximation quality. QPLEX [34] further refines the decomposition by adopting a duplex dueling architecture that satisfies the Individual-Global-Max (IGM) principle via an advantage-based formulation. Despite their improvements in expressiveness, these methods primarily focus on functional accuracy and provide little insight into the underlying coordination structure. This lack of interpretability becomes particularly problematic in partially observable and interaction-intensive environments, where understanding agent dependencies is crucial for robust credit assignment. To address this, we propose a novel interpretable value decomposition framework that explicitly encodes high-order interactions, offering both performance and transparency.

Interpretable MARL. Recent advances in interpretable MARL can be broadly categorized into two paradigms, focusing either on (i) intrinsic interpretability or (ii) post-hoc explanation [43]. Intrinsic interpretability requires the learned model to be self-understandable by nature, which is achieved by using a transparent class of models, whereas post-hoc explanation entails learning a second model to explain an already-trained black-box model. Post-hoc methods provide auxiliary insights without modifying the underlying learning process. For instance, SQDDPG [12] estimates individual agent contributions via Shapley Q-values, while Goto et al. [13] use masked-attention to identify salient observation regions in multi-vehicle coordination tasks. Although informative, these techniques lack robustness guarantees and struggle to recover the relational or temporal structure intrinsic to multi-agent cooperation. In contrast, intrinsically interpretable approaches seek to construct models whose decision logic is understandable by design. Tree-based architectures such as MIXRT [15] and MAVIPER [14] represent agent policies using soft or symbolic decision trees, providing explicit reasoning paths. DTPO [16] advances this line by directly optimizing tree structures via policy gradients, combining transparency with performance. Attention-based models, such as MAAC [44], further enhance interpretability by dynamically identifying inter-agent dependencies, while other methods promote explainability through latent skill inference [45] or constrained policy spaces that encode global objectives [46].

Within the value decomposition framework, central to cooperative MARL, several works also try to understand how agents cooperate via agent-level contributions. VDN [21] factorizes the team reward additively, assuming agent independence. SHAQ [37] adopts Shapley value theory to quantify marginal contributions across coalitions. More recently, NA^2Q [22] expands the joint value function via a Taylor-like decomposition to capture high-order interactions. However, such expansions scale exponentially with the number of agents, leading to substantial computational and interpretability challenges. These limitations highlight the need for a more principled and scalable formulation that can compactly model high-order agent interactions without sacrificing transparency. To this end, we propose a novel approach that integrates continued fraction networks into the value decomposition framework. By leveraging the recursive structure of continued fractions, our method enables compact and interpretable representations of arbitrary-order interactions while maintaining linear complexity with respect to the number of agents. This formulation provides a powerful alternative to polynomial expansion-based methods, offering both expressive capacity and interpretability in large-scale cooperative MARL settings.

B Proof

B.1 Objective Functions for Variational Information Bottlenecks

Considering the Markov chain $\mathbf{u}^* \leftrightarrow \mathbf{h} \leftrightarrow \mathbf{m}$, which means the assistive information cannot depend directly on the \mathbf{u}^* . So we have $p(\mathbf{m} | \mathbf{h}, \mathbf{u}^*) = p(\mathbf{m} | \mathbf{h})$.

As in the IB, the objective can be written as:

$$J_{IB}(\phi) = I(\mathbf{m}, \mathbf{u}^*; \phi) - \beta I(\mathbf{m}, \mathbf{h}; \phi). \quad (15)$$

The β is to realize the trade-off between a succinct representation and inferencing ability.

Theorem 1 (Lower Bound for $I(\mathbf{m}, \mathbf{u}^*; \phi)$). *Let the representation m_i be reparameterized as a random variable drawn from a multivariate Gaussian distribution $m_i \sim \mathcal{N}(f_m(h_i; \phi_m), \mathbf{I})$, where f_m is an encoder parameterized by ϕ_m , h_i denotes the hidden state of agent i , and \mathbf{I} is the identity covariance matrix. Then, the mutual information between the assistive information \mathbf{m} and the optimal joint action \mathbf{u}^* is lower-bounded as:*

$$I(\mathbf{m}, \mathbf{u}^*; \phi) \geq \frac{1}{N} \sum_{i=1}^N \mathbb{E}_{\epsilon \sim p(\epsilon)} [-\log q(u_i^* | f(h_i, \epsilon))], \quad (16)$$

where $q(u_i^* | m_i)$ is a variational distribution approximating the true posterior $p(u_i^* | m_i)$, and $m_i = f(h_i, \epsilon)$ denotes a deterministic function of h_i and the Gaussian random variable ϵ .

Proof.

$$\begin{aligned} I(\mathbf{m}, \mathbf{u}^*; \phi) &= \int dm_i du_i^* p(m_i, u_i^*) \log \frac{p(m_i, u_i^*)}{p(m_i) p(u_i^*)} \\ &= \int dm_i du_i^* p(m_i, u_i^*) \log \frac{p(u_i^* | m_i)}{p(u_i^*)}, \end{aligned}$$

where $p(u_i^* | m_i)$ is fully defined by our encoder and Markov Chain as follows:

$$\begin{aligned} p(u_i^* | m_i) &= \int dh_i p(h_i, u_i^* | m_i) \\ &= \int dh_i p(u_i^* | h_i) p(h_i | m_i) \\ &= \int dh_i \frac{p(u_i^* | h_i) p(m_i | h_i) p(h_i)}{p(m_i)}. \end{aligned}$$

Since this is intractable in our case, let $q(u_i^* | m_i)$ be a variational approximation to $p(u_i^* | m_i)$, where this is our decoder which we will take to another neural network with its own set of parameters. Using the fact that Kullback Leibler divergence is always positive, we have

$$\begin{aligned} \text{KL}[p(u_i^* | m_i), q(u_i^* | m_i)] &\geq 0 \\ \implies \int du_i^* p(u_i^* | m_i) \log p(u_i^* | m_i) &\geq \int du_i^* p(u_i^* | m_i) \log q(u_i^* | m_i), \end{aligned}$$

and hence

$$\begin{aligned} I(\mathbf{m}, \mathbf{u}^*; \phi) &\geq \int du_i^* dm_i p(u_i^*, m_i) \log \frac{q(u_i^* | m_i)}{p(u_i^*)} \\ &= \int du_i^* dm_i p(u_i^*, m_i) \log q(u_i^* | m_i) - \int du_i^* p(u_i^*) \log p(u_i^*) \\ &= \int du_i^* dm_i p(u_i^*, m_i) \log q(u_i^* | m_i) + H(u_i^*) \\ &= \int dh_i du_i^* dm_i p(h_i) p(u_i^* | h_i) p(m_i | h_i) \log q(u_i^* | m_i) + H(u_i^*) \\ &= \frac{1}{N} \sum_{i=1}^N \left[\int dm_i p(m_i | \tau_i) \log q(u_i^* | m_i) \right] + H(u_i^*). \end{aligned}$$

Notice that the entropy of our labels $H(u_i^*)$ is independent of our optimization procedure and so can be ignored. And as we can rewrite $p(m_i | h_i) dm_i = p(\epsilon) d\epsilon$, $m_i = f(h_i, \epsilon)$. So we have

$$I(\mathbf{m}, \mathbf{u}^*; \phi) \geq \frac{1}{N} \sum_{i=1}^N \mathbb{E}_{\epsilon \sim p(\epsilon)} [-\log q(u_i^* | f(h_i, \epsilon))].$$

□

Theorem 2 (Upper Bound for $I(\mathbf{m}, \mathbf{h}; \phi)$). *Let $\tilde{q}(\mathbf{m})$ denote a variational approximation of the marginal distribution $p(\mathbf{m})$. Then, the mutual information between the representation \mathbf{m} and the hidden state \mathbf{h} admits the following upper bound:*

$$I(\mathbf{m}, \mathbf{h}; \phi) \leq \text{KL}(p(\mathbf{m} | h_i) \| \tilde{q}(\mathbf{m})). \quad (17)$$

Proof.

$$\begin{aligned} I(\mathbf{m}, \mathbf{h}; \phi) &= \int dm_i dh_i p(h_i, m_i) \log \frac{p(m_i | h_i)}{p(m_i)} \\ &= \int dm_i dh_i p(h_i, m_i) \log p(m_i | h_i) - \int dm_i p(m_i) \log p(m_i). \end{aligned}$$

Let $\tilde{q}(m_i)$ be the variational approximation to the marginal distribution $p(m_i) = \int dh_i p(m_i | h_i) p(h_i)$. Since $\text{KL}[p(m_i), \tilde{q}(m_i)] \geq 0 \implies \int dm_i p(m_i) \log p(m_i) \geq \int dm_i p(m_i) \log \tilde{q}(m_i)$, we have

$$\begin{aligned} I(\mathbf{m}, \mathbf{h}; \phi) &\leq \int dh_i dm_i p(h_i) p(m_i | h_i) \log \frac{p(m_i | h_i)}{\tilde{q}(m_i)} \\ &= \frac{1}{N} \sum_{i=1}^N \left[p(m_i | h_i) \log \frac{p(m_i | h_i)}{\tilde{q}(m_i)} \right] \\ &= \text{KL}[p(\mathbf{m} | h_i), \tilde{q}(\mathbf{m})]. \end{aligned}$$

□

Combining *Theorem 1* and *Theorem 2*, we have the objective functions for variational information bottlenecks, which is to minimize

$$\mathcal{L}_{VIB} = \frac{1}{N} \sum_{i=1}^N \mathbb{E}_{\epsilon \sim p(\epsilon)} [-\log q(u_i^* | f(h_i, \epsilon))] + \beta \text{KL}[p(\mathbf{m} | h_i), \tilde{q}(\mathbf{m})]. \quad (18)$$

B.2 Correspondence between Continued Fraction Depth and the Order of Agent Interactions

In this section, we establish a one-to-one correspondence between the depth d of the continued fraction network and the order of agent interactions. This property allows the d -th order continued fraction to accurately represent the d -th order approximation of the agent's behavior.

Specifically, a continued fraction network of depth d , $\frac{1}{w_1 Q + \frac{1}{w_2 Q + \frac{1}{w_3 Q + \dots \frac{1}{w_d Q}}}}$ can be reformulated as $f(Q) = T_d(Q) + \mathcal{O}_{d+1}(Q)$, where $T_n(Q)$ is a degree- d polynomial of Q , and $\mathcal{O}_{d+1}(Q)$ denotes terms of order $d+1$ or higher in Q .

By setting $z = \frac{1}{Q}$, the continued fraction $\frac{1}{w_1 Q + \frac{1}{w_2 Q + \frac{1}{w_3 Q + \dots \frac{1}{w_d Q}}}}$ can be transformed into

$$\mathbf{K}(z) = \frac{z}{w_1} \frac{z}{w_2} \frac{z}{w_3 + \dots}, \quad (19)$$

since these approximants are arranged along the "staircase diagonals" of the Padé table.

Theorem 3. *For the d -th order truncation of the continued fraction $R_k(z) = \frac{A_k(z)}{B_k(z)}$, the following holds:*

$$p_d = \left\lfloor \frac{d+1}{2} \right\rfloor, \quad q_d = \left\lfloor \frac{d}{2} \right\rfloor, \quad (20)$$

where $p_d = \deg(A_d)$, $q_d = \deg(B_d)$.

Proof. The k -th order asymptotic function $\frac{A_k(z)}{B_k(z)}$ satisfies the recursive relations:

$$\begin{cases} A_k(z) = \mathbf{w}_k A_{k-1}(z) + z A_{k-2}(z) \\ B_k(z) = \mathbf{w}_k B_{k-1}(z) + z B_{k-2}(z) \end{cases},$$

with

$$\begin{bmatrix} A_{-1} & A_0 \\ B_{-1} & B_0 \end{bmatrix} = \begin{bmatrix} 1 & 0 \\ 0 & 1 \end{bmatrix}.$$

Assume that for all $k \leq n$, the following holds:

$$\deg(A_k) = \left\lfloor \frac{k+1}{2} \right\rfloor, \quad \deg(B_k) = \left\lfloor \frac{k}{2} \right\rfloor.$$

Base Cases:

$n = 1$:

$$A_1(z) = \mathbf{w}_1 A_0(z) + z A_{-1}(z) = z \Rightarrow \deg(A_1) = 1, \quad \left\lfloor \frac{1+1}{2} \right\rfloor = 1.$$

$$B_1(z) = \mathbf{w}_1 B_0(z) + z B_{-1}(z) = \mathbf{w}_1 \Rightarrow \deg(B_1) = 0, \quad \left\lfloor \frac{1}{2} \right\rfloor = 0.$$

$n = 2$:

$$A_2(z) = \mathbf{w}_2 A_1(z) + z A_0(z) = \mathbf{w}_2 z \Rightarrow \deg(A_2) = 1, \quad \left\lfloor \frac{3}{2} \right\rfloor = 1.$$

$$B_2(z) = \mathbf{w}_2 B_1(z) + z B_0(z) = \mathbf{w}_1 \mathbf{w}_2 + z \Rightarrow \deg(B_2) = 1, \quad \left\lfloor \frac{2}{2} \right\rfloor = 1.$$

Hence, the base cases hold.

Then assume the statements hold for $k = n - 1$ and $k = n - 2$, and prove that they also hold for $k = n$.

Degree of the Numerator $A_n(z)$:

From the recurrence:

$$A_n(z) = \mathbf{w}_n A_{n-1}(z) + z A_{n-2}(z),$$

and by the induction hypothesis:

$$\deg(A_{n-1}) = \left\lfloor \frac{n}{2} \right\rfloor, \quad \deg(A_{n-2}) = \left\lfloor \frac{n-1}{2} \right\rfloor.$$

Then:

$$\deg(\mathbf{w}_n A_{n-1}) = \left\lfloor \frac{n}{2} \right\rfloor, \quad \deg(z A_{n-2}) = 1 + \left\lfloor \frac{n-1}{2} \right\rfloor.$$

Case 1: n even, let $n = 2m$:

$$\left\lfloor \frac{n}{2} \right\rfloor = m, \quad \left\lfloor \frac{n-1}{2} \right\rfloor = m - 1.$$

Then

$$\deg(\mathbf{w}_n A_{n-1}) = m, \quad \deg(z A_{n-2}) = 1 + (m - 1) = m \Rightarrow \deg(A_n) = m = \left\lfloor \frac{n+1}{2} \right\rfloor.$$

Case 2: n odd, let $n = 2m + 1$:

$$\left\lfloor \frac{n}{2} \right\rfloor = m, \quad \left\lfloor \frac{n-1}{2} \right\rfloor = m.$$

Then

$$\deg(\mathbf{w}_n A_{n-1}) = m, \quad \deg(z A_{n-2}) = 1 + m = m + 1 \Rightarrow \deg(A_n) = m + 1 = \left\lfloor \frac{n+1}{2} \right\rfloor.$$

Degree of the Denominator $B_n(z)$:

From the recurrence:

$$B_n(z) = w_n B_{n-1}(z) + z B_{n-2}(z),$$

and using the induction hypothesis:

$$\deg(B_{n-1}) = \left\lfloor \frac{n-1}{2} \right\rfloor, \quad \deg(B_{n-2}) = \left\lfloor \frac{n-2}{2} \right\rfloor.$$

Then:

$$\deg(w_n B_{n-1}) = \left\lfloor \frac{n-1}{2} \right\rfloor, \quad \deg(z B_{n-2}) = 1 + \left\lfloor \frac{n-2}{2} \right\rfloor.$$

Case 1: $n = 2m$ (even):

$$\left\lfloor \frac{n-1}{2} \right\rfloor = m-1, \quad \left\lfloor \frac{n-2}{2} \right\rfloor = m-1.$$

Then

$$\deg(w_n B_{n-1}) = m-1, \quad \deg(z B_{n-2}) = m \Rightarrow \deg(B_n) = m = \left\lfloor \frac{n}{2} \right\rfloor.$$

Case 2: $n = 2m+1$ (odd):

$$\left\lfloor \frac{n-1}{2} \right\rfloor = m, \quad \left\lfloor \frac{n-2}{2} \right\rfloor = m-1.$$

Then

$$\deg(w_n B_{n-1}) = m, \quad \deg(z B_{n-2}) = m \Rightarrow \deg(B_n) = m = \left\lfloor \frac{n}{2} \right\rfloor.$$

By mathematical induction, we conclude that:

$$\deg(A_n) = \left\lfloor \frac{n+1}{2} \right\rfloor, \quad \deg(B_n) = \left\lfloor \frac{n}{2} \right\rfloor.$$

Therefore, when the truncation order is $n = d$, we have

$$p_d = \left\lfloor \frac{d+1}{2} \right\rfloor, \quad q_d = \left\lfloor \frac{d}{2} \right\rfloor.$$

□

Theorem 4. *The d -th order truncation of the continued fraction $R_d(z) = \frac{A_d(z)}{B_d(z)}$ naturally satisfies the conditions for a Padé approximant, specifically:*

$$f(z) - R_d(z) = \mathcal{O}(z^{p_d+q_d+1}), \quad (21)$$

which means that its Taylor expansion coincides with the first d terms of the original function $f(z)$.

Proof.

Definition 1 (Padé Approximant [25, 26]). *Let $C(z) = \sum_{k=0}^{\infty} c_k z^k$ be a formal power series in the variable z , then the Padé approximant of order $[L/M]$ is a rational function of the form:*

$$R_{L,M}(z) = [A_{L,M}(z)]/[B_{L,M}(z)], \quad (22)$$

where $A_{L,M}(z)$ and $B_{L,M}(z)$ are polynomials of degrees at most L and M , respectively, chosen such that

$$B_{L,M}(z)C(z) - A_{L,M}(z) = \mathcal{O}(z^{L+M+1}), \quad (23)$$

where notation $\mathcal{O}(z^k)$ denotes some power series of the form $\sum_{n=k}^{\infty} \tilde{c}_n z^n$. This approximation minimizes the difference between the rational function and the power series up to the order $L+M$.

Since $R_d(z) = \frac{A_d(z)}{B_d(z)}$, we have

$$f(z) - \frac{A_d(z)}{B_d(z)} = \mathcal{O}(z^{p_d+q_d+1}), \quad (24)$$

which implies

$$f(z)B_d(z) - A_d(z) = \mathcal{O}(z^{p_d+q_d+1})B_d(z) = \mathcal{O}(z^{p_d+q_d+1}). \quad (25)$$

Lemma 1. For all $k \geq 0$, there exists a polynomial $S_k(z)$ such that:

$$f(z)B_k(z) - A_k(z) = (-1)^k z^{k+1} S_k(z), \quad (26)$$

and the constant term $S_k(0) \neq 0$.

Proof. We can prove this lemma by mathematical induction.

Base Case:

$k = 0$:

$$f(z)B_0(z) - A_0(z) = f(z) \cdot 1 - 0 = f(z).$$

By the definition of continued fractions, $f(z) = \frac{z}{a_1 + \dots}$, so:

$$f(z) = z \cdot (\text{analytic function}) = zS_0(z), \quad S_0(0) = \frac{1}{a_1} \neq 0.$$

Inductive Hypothesis ($k - 1$ and $k - 2$ hold):

$$\begin{aligned} f(z)B_{k-1}(z) - A_{k-1}(z) &= (-1)^{k-1} z^k S_{k-1}(z) \\ f(z)B_{k-2}(z) - A_{k-2}(z) &= (-1)^{k-2} z^{k-1} S_{k-2}(z) \end{aligned}$$

for k :

Substituting the recurrence relations:

$$\begin{aligned} f(z)B_k(z) - A_k(z) &= f(z)(\mathbf{w}_k B_{k-1}(z) + zB_{k-2}(z)) - (\mathbf{w}_k A_{k-1}(z) + zA_{k-2}(z)) \\ &= \mathbf{w}_k (f(z)B_{k-1}(z) - A_{k-1}(z)) + z(f(z)B_{k-2}(z) - A_{k-2}(z)) \\ &= \mathbf{w}_k (-1)^{k-1} z^k S_{k-1}(z) + z(-1)^{k-2} z^{k-1} S_{k-2}(z) \\ &= (-1)^k z^k (-\mathbf{w}_k S_{k-1}(z) + S_{k-2}(z)) \\ &= (-1)^k z^{k+1} S_k(z), \end{aligned}$$

where $S_k(z)$ is the polynomial obtained from $-\mathbf{w}_k S_{k-1}(z) + S_{k-2}(z)$, divided by z . \square

From the lemma, we have:

$$f(z) - \frac{A_d(z)}{B_d(z)} = \frac{f(z)B_d(z) - A_d(z)}{B_d(z)} = \frac{(-1)^d z^{d+1} S_d(z)}{B_d(z)}.$$

Since $B_d(0) = \mathbf{w}_1 \mathbf{w}_2 \cdots \mathbf{w}_d \neq 0$ (assuming $w_k \neq 0$) and $S_d(0) \neq 0$, it follows that:

$$f(z) - R_d(z) = \mathcal{O}(z^{d+1}).$$

According to *Theorem 3*, the degree of the numerator $A_d(z)$ is $p_d = \lfloor \frac{d+1}{2} \rfloor$, and the degree of the denominator $B_d(z)$ is $q_d = \lfloor \frac{d}{2} \rfloor$. When d is odd, we have $p_d = q_d = \frac{d}{2}$; when d is even, $p_d = \frac{d+1}{2}$, $q_d = \frac{d-1}{2}$. In both cases, it follows that $p_d + q_d = d$. Therefore,

$$f(z) - R_d(z) = \mathcal{O}(z^{d+1}) = \mathcal{O}(z^{p_d+q_d+1}),$$

which satisfies the condition of a Padé approximant. \square

In conclusion, the depth- d continued fraction network represents the d -th order truncation of the continued fraction:

$$\frac{1}{\mathbf{w}_1 Q +} \frac{1}{\mathbf{w}_2 Q +} \cdots \frac{1}{\mathbf{w}_d Q},$$

which forms a $[p_d, q_d]$ -Padé approximant with $p_d + q_d = d$. This enables accurate representation of the first d -th order interactions among agents.

C Experimental Details

C.1 Algorithmic Description

Algorithm 1 Continued Fraction Q-Learning

- 1: Initialize environment, agent network $Q_i(\tau_i, u_i; \theta)$, target network $Q_i(\tau'_i, u'_i; \hat{\theta})$, mixing network Q_{tot} , and VIB module $G_\phi(E_{\phi_1}, D_{\phi_2})$
 - 2: Initialize replay buffer \mathcal{D}
 - 3: **repeat**
 - 4: Obtain the initial global state s^0
 - 5: **for** $t = 0$ to $T - 1$ **do**
 - 6: For each agent i , get action-observation history τ_i^t
 - 7: Calculate individual value function Q_i
 - 8: Get the hidden state h_i^t
 - 9: Select action u_i^t via value function with probability ϵ exploration
 - 10: Execute joint action \mathbf{u}^t , receive reward r^t , next state s^{t+1}
 - 11: **end for**
 - 12: Store the episode trajectory in \mathcal{D}
 - 13: Sample a mini-batch \mathcal{B} of size b from \mathcal{D}
 - 14: **for** $t = 0$ to $T - 1$ **do**
 - 15: Calculate $\mu, \sigma = E_{\phi_1}(h_i^t)$
 - 16: Generate assistive information \mathbf{m}
 - 17: Get the attention weight α_k by the intervention function in Eq. 12
 - 18: Calculate the joint value function Q_{tot}
 - 19: **end for**
 - 20: Calculate loss $\mathcal{L}(\theta) = \mathcal{L}_{Q_{tot}} + \mathcal{L}_{VIB}$ via Eq. 11 and Eq. 14.
 - 21: Update ϕ and θ by minimizing the above loss
 - 22: Periodically update $\hat{\theta} \leftarrow \theta$
 - 23: **until** $Q_i(\tau_i, u_i; \theta)$ converges or maximum steps reached
-

C.2 LBF Description and Hyperparameters Settings

Level-Based Foraging (LBF) [31] is a mixed cooperative-competitive MARL benchmark, where each agent navigates a 10×10 grid world. Agents and food items are randomly placed in a 2D grid, and each one is assigned a level. A food item can only be collected when the combined levels of all participating agents equal or exceed its level. The environment induces a spectrum of collaborative behaviors through its level-dependent reward structure: while low-level food items permit independent collection, higher-level resources necessitate coalition formation. Furthermore, we set the penalty reward for movement to -0.002 , and the detailed hyperparameter settings of LBF are shown in Table 1.

Observation Space. Each agent observes a 2×2 square grid centered on its own position. Within this range, the agent receives a structured array containing the (x, y) coordinates and levels of all visible food items and other agents. This observation provides both spatial and attribute-level information to support localized decision-making.

Action Space. The discrete action space for each agent consists of none, move [direction], and load food. Each agent only moves into one unoccupied grid. If multiple agents attempt to move into the same grid, collisions are resolved by canceling the conflicting moves, leaving the agents in their original positions.

Table 1: The configurations of LBF.

Hyperparameter	Value
Max Episode Length	50
Batch Size	32
Test Interval	10000
Test Episodes	32
Replay Batch Size	5000
Discount Factor	0.99
Start Exploration Rate	1.0
End Exploration Rate	0.05
Anneal Steps	50000
Steps	1M
Target Update Interval	200

Rewards. This reward depends on the food’s level, which is distributed among the participating agents in proportion based on their levels. The rewards are normalized to maintain a unit sum across all agents. This design ensures contribution-based fairness in reward distribution while enhancing cooperative efficiency among agents.

C.3 StarCraft II Description and Hyperparameters Settings

All implementations of algorithms are conducted on StarCraft II unit micro-management tasks (SC2.4.10). We evaluate performance in combat scenarios where enemy units are controlled by the built-in AI with the *difficulty=7* setting, and each allied unit is controlled by the decentralized agents with reinforcement learning algorithms. During battles, the agents seek to maximize the damage dealt to enemy units while minimizing damage received, requiring the coordination of diverse tactical skills. We assess our method across a variety of challenging scenarios that differ in terms of symmetry, agent composition, and unit count (as shown in Table 3). For clarity, we also outline the core settings of the StarCraft Multi-Agent Challenge (SMAC) [32], including observation, state, action, and reward configurations. The detailed hyperparameter settings of SMAC are shown in Table 2.

Table 2: The configurations of SMAC.

Hyperparameter	Value
Difficulty	7
Batch Size	32
Test Interval	10000
Test Episodes	32
Replay Batch Size	5000
Discount Factor	0.99
Start Exploration Rate	1.0
End Exploration Rate	0.05
Target Update Interval	200
Optimizer	RMSprop
Learning Rate	0.0005

Observations and States. At each time step, each agent receives a local observation of units within its field of view. The observation includes the following features for both allied and enemy units: distance, relative X and Y positions, health, shield, and unit type. Note that the agents can only observe the others if they are alive and within their line of sight range, which is set to 9. When a unit (ally or enemy) becomes invisible or is eliminated, its feature vector is reset to all zeros, indicating either death or being outside the field of view. The global state is only available during centralized training, which contains information about all units on the map. Finally, all features, including the global state and the observation of the agent, are normalized by their maximum values.

Action Space. Each unit takes an action from the discrete action set: no-op, stop, move [direction], and attack [enemy id]. Agents are allowed to move with a fixed movement amount in four directions: north, south, east, and west, where the unit is allowed to take the attack [enemy id] action only when the enemy is within its shooting range.

Rewards. The target goal is to maximize the win rate for each battle scenario. At each time step, the agents receive a shaped reward based on the hit-point damage dealt and enemy units killed, as well as a special bonus for winning the battle. Additionally, agents obtain a 10 positive bonus after killing each enemy and a 200 bonus when killing all enemies, which is consistent with the default reward function of the SMAC.

Table 3: The StarCraft Multi-Agent Challenge benchmark.

Map	Ally Units	Enemy Units	Difficulty	Steps	Anneal Steps	<i>d</i>
2s3z	2 Stalkers, 3 Zealots	2 Stalkers, 3 Zealots	Eazy	1.5M	50000	2
2c_vs_64zg	2 Colossus	64 Zerglings	Hard	2M	50000	2
3s_vs_5z	3 Stalkers	5 Zealots	Hard	2M	50000	2
5m_vs_6m	5 Marines	6 Marines	Hard	2M	50000	4
3s5z_vs_3s6z	3 Stalkers, 5 Zealots	3 Stalkers, 6 Zealots	Super Hard	5M	200000	6
6h_vs_8z	6 Hydralisks	8 Zealots	Super Hard	5M	200000	6

C.4 SMACv2 Description and Hyperparameters Settings

SMACv2 [33] is an enhanced benchmark for cooperative multi-agent reinforcement learning built on top of StarCraft II. It preserves the original SMAC API while introducing three procedural innovations to increase scenario diversity and challenge contemporary MARL algorithms: randomising start positions, randomising unit types, and changing the unit sight and attack ranges.

Randomized Start Positions. Allied and enemy units are spawned either in a "surround" configuration, where enemies encircle the allies, or via a "reflect" scheme that mirrors allied positions across the map center. This ensures that agents cannot overfit to fixed spawn patterns.

Randomized Unit Types. Each battle can feature mixed unit compositions rather than uniform rosters. For Terran, Protoss, and Zerg, three unit types are sampled with configurable probabilities through the `team_gen` distribution (as shown in Table 4), promoting adaptable strategies under varied team makeups.

Unit Sight and Attack Ranges. Unit vision cones and attack radii are aligned with their true in-game values, increasing realism and preventing agents from exploiting the simplified ranges used in SMAC.

Table 4: The configurations of SMACv2.

Race	Unit	probability
Protoss	Stalker	0.45
	Zealot	0.45
	Colossus	0.1
Terran	Marine	0.45
	Marauder	0.45
	Medivac	0.1
Zerg	Zergling	0.45
	Hydralisk	0.45
	Baneling	0.1

C.5 Implementation Details

We compare our method against nine value-based baselines, including VDN [21], QMIX [11], QPLEX [34], Centrally-Weighted QMIX (CW-QMIX) [35], CDS [36], SHAQ [37], GoMARL [38], ReBorn [39], and NA²Q [22]. To ensure fairness, we implement all experiments within the PyMARL framework². All hyperparameters of baselines are set identically to our method to compare algorithms fairly. Please refer to PyMARL’s open-source implementation for further training details and fair comparison settings. The depth d of CFN is determined based on the scale of agents and the complexity of each task.

All scenarios are trained on a system equipped with an NVIDIA RTX 3080TI GPU and an Intel i9-12900k CPU, with training time ranging from 1 to 16 hours per scenario, depending on the task complexity and episode length.

²The source code of implementations is from <https://github.com/oxwhirl/pymarl>.

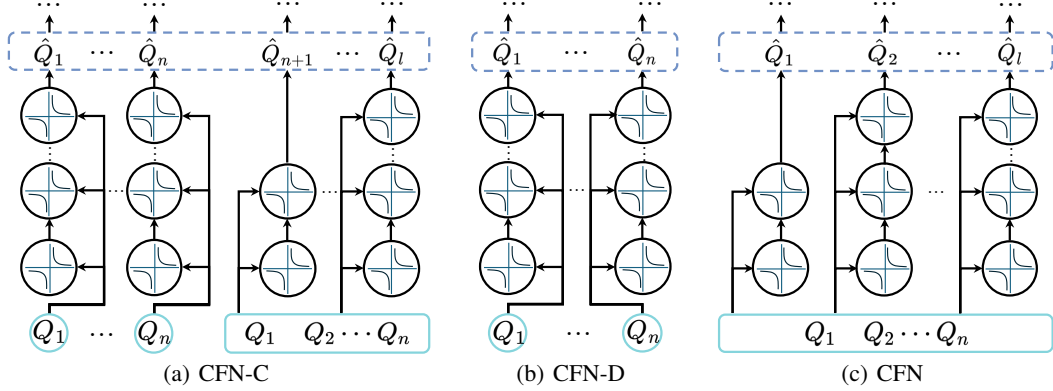


Figure 10: Three variants of the CFN architecture. (a) CFN-C integrates both single-feature ladders, where each ladder processes a single input dimension Q_i , and full ladders, which take the complete set of individual values Q as input. (b) CFN-D utilizes only the single-feature ladders. (c) CFN employs only the full ladders with increasing depth.

C.6 Detailed Description of CFN Structure

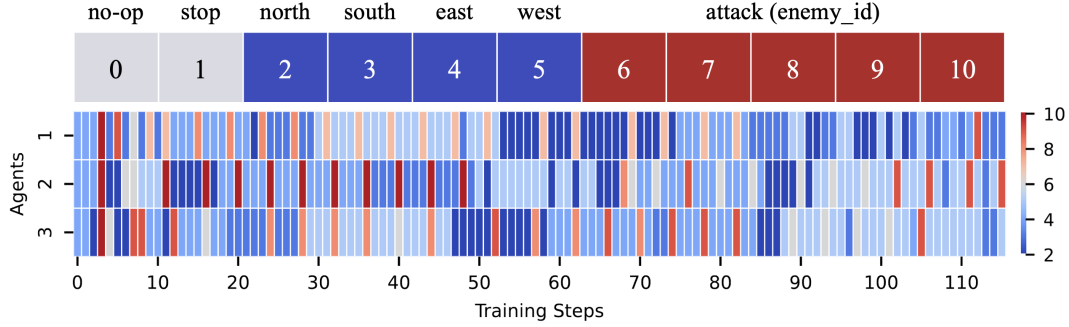
As illustrated in *Fig. 10*, the CFN framework includes two structural variants in addition to the main architecture. *Fig. 10(a)* presents CFN-C, a composite architecture inspired by CoFrNet [18], which combines two types of ladders: single-feature ladders, each processing an individual agent utility Q_i , and full-input ladders, which receive the complete utility vector Q at every layer. Each ladder yields a partial joint value \hat{Q}_k , and the aggregation of all ladders constitutes the final joint Q-value.

The number of single-feature ladders equals the number of agents, enabling additive modeling of individual effects. In contrast, full-input ladders are deeper and designed to capture complex joint dependencies among agents by recursively combining all inputs, thereby facilitating high-order interaction modeling.

Fig. 10(b) and *Fig. 10(c)* depict two simplified variants: 1) CFN-D, which retains only the single-feature ladders, thereby modeling additive effects with strong transparency [47] but lacking the capacity to express inter-agent interactions; 2) CFN, which retains only the full-input ladders, striking a balance between modeling power and computational efficiency.

In our QCoFr algorithm, we adopt the CFN structure with full-input ladders as the default architecture. Compared to CFN-C, this version significantly reduces parameter overhead while preserving the ability to capture arbitrary-order interactions. We further include CFN-D as an ablation baseline to isolate the contribution of high-order modeling: while CFN-D offers interpretability due to its decomposable additive form, its inability to encode dependencies across agents limits its expressiveness in cooperative settings.

Finally, a key advantage of the CFN structure is its linear scalability: the number of parameters grows as $\mathcal{O}(n)$ with the number of agents, making it particularly suited to large-scale MARL scenarios where modeling expressive joint behavior is critical without incurring prohibitive computational costs.



(a) Actions of each agent.



(b) $t = 25$



(c) $t = 75$



(d) $t = 85$



(e) $t = 100$

Figure 11: Visualization of evaluation results for QCoFr on $3s_vs_5z$ map. Agents demonstrate a coordinated kite-and-focus-fire strategy: agent 2 initially kites four enemies alone, while agent 1 and agent 3 eliminate another. Agent 3 then draws away two of the remaining enemies, enabling agent 1 and agent 2 to dispatch the others. Finally, all agents regroup to defeat the last enemies.

D Extended Interpretability Analysis

Fig. 11 illustrates the interpretability of QCoFr on $3s_vs_5z$ scenario. At the beginning of the episode, agent 2 independently kites four enemies, creating a numerical advantage that enables agent 1 and agent 3 to quickly eliminate an isolated opponent. As a result, agent 2 receives the highest individual contribution score (1.337), while the strongest pairwise contribution is observed between agents 1 and 3 due to their effective coordination. As the engagement progresses, agent 3 draws two enemies away, allowing agent 1 and agent 2 to jointly take down the remaining targets. During this phase, the coalition contribution of agents 1 and 2 increases, and agent 3's individual contribution also rises as it delays the enemy. After these enemies are defeated, all three agents regroup to focus fire on the remaining units, resulting in a more balanced distribution of credit across agents. This case study demonstrates that the agents have learned a kite-and-focus-fire strategy. The alignment between observed behaviors and quantitative contribution values confirms the interpretability of QCoFr, which faithfully attributes both individual and coalition-level contributions with high-order interactions in executing complex cooperative tactics.

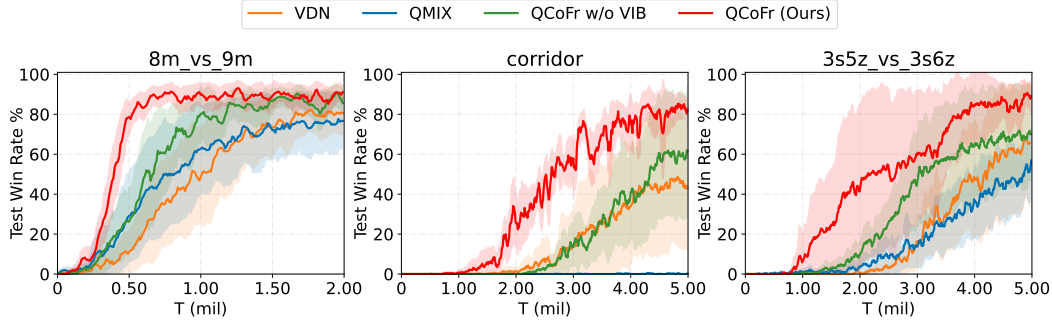


Figure 12: Performance with and without VIB on three extra scenarios of the SMAC benchmark.

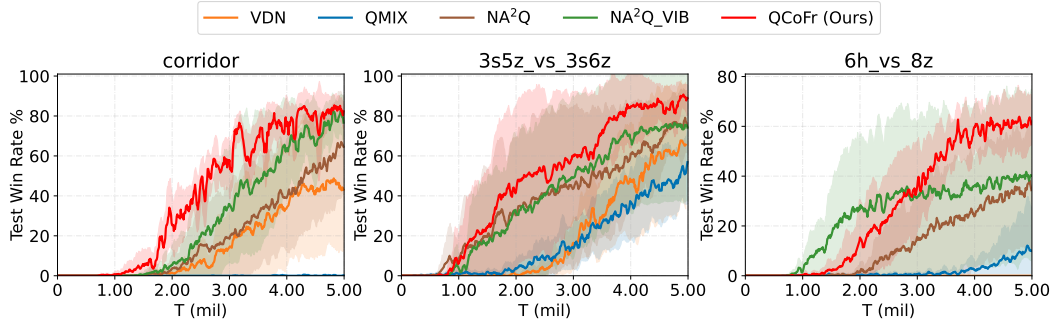


Figure 13: Performance comparison of NA^2Q with the VIB module and our method.

E Additional Experiments on SMAC

E.1 Additional Ablation Experiments

The Role of the VIB Module. We ablate the VIB component on three additional SMAC scenarios (Fig. 12), comparing QCoFr with and without VIB under identical settings. With VIB, QCoFr consistently accelerates early learning and achieves higher test win rates, confirming that task-relevant assistive information improves credit assignment and coordination.

The Role of CFN. Since NA^2Q struggles to model higher-order interactions, we equip it with the same VIB module and evaluate on three super-hard SMAC maps, comparing against QCoFr (Fig. 13). This isolates the effect of interaction modeling from that of assistive information. While NA^2Q+VIB outperforms the original NA^2Q , a clear gap remains to QCoFr. The results indicate that, on complex tasks, explicitly modeling higher-order dependencies enables more refined cooperative strategies, which highlights the effectiveness of the CFN module beyond what VIB alone can provide.

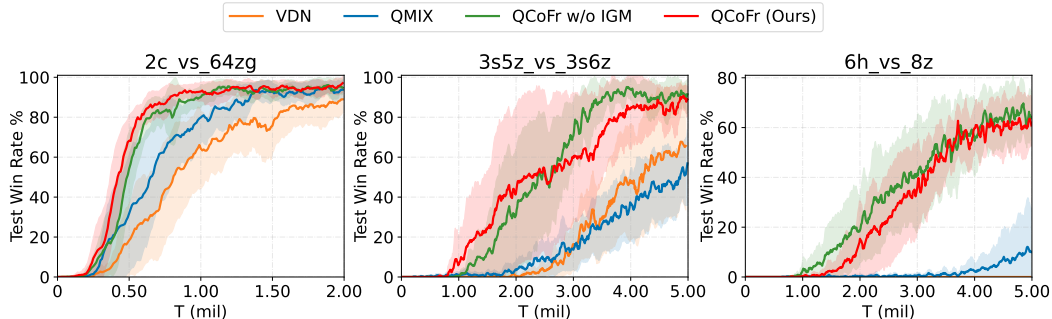


Figure 14: Performance comparison of QCoFr with and without IGM constraint.

E.2 Discussion on the IGM Constraint

To isolate the effect of the continued-fraction mixing paradigm from non-monotonic joint-action search, we enforce the Individual-Global-Max (IGM) constraint in our framework. Notably, the universal approximation theorem applies to any linear combination of continued fractions and does not require non-negative weights [18], suggesting that the approach can be extended to non-IGM mixers. Integrating CFN with fully IGM-free methods such as DAVE [48] is therefore a natural direction. DAVE emphasizes that most value decomposition methods operate under IGM, which couples the optimal joint action with the optimal individual actions. Relaxing this constraint requires agents to explicitly search for the globally optimal joint action at execution time, often via an auxiliary network. To probe this possibility, we conduct experiments under relaxed IGM assumptions on three SMAC scenarios. As shown in *Fig. 14*, QCoFr achieves comparable or even slightly improved performance without IGM, indicating that our architecture can still recover high-quality joint actions.

NeurIPS Paper Checklist

The checklist is designed to encourage best practices for responsible machine learning research, addressing issues of reproducibility, transparency, research ethics, and societal impact. Do not remove the checklist: **The papers not including the checklist will be desk rejected.** The checklist should follow the references and follow the (optional) supplemental material. The checklist does NOT count towards the page limit.

Please read the checklist guidelines carefully for information on how to answer these questions. For each question in the checklist:

- You should answer [Yes], [No], or [NA].
- [NA] means either that the question is Not Applicable for that particular paper or the relevant information is Not Available.
- Please provide a short (1-2 sentence) justification right after your answer (even for NA).

The checklist answers are an integral part of your paper submission. They are visible to the reviewers, area chairs, senior area chairs, and ethics reviewers. You will be asked to also include it (after eventual revisions) with the final version of your paper, and its final version will be published with the paper.

The reviewers of your paper will be asked to use the checklist as one of the factors in their evaluation. While "[Yes]" is generally preferable to "[No]", it is perfectly acceptable to answer "[No]" provided a proper justification is given (e.g., "error bars are not reported because it would be too computationally expensive" or "we were unable to find the license for the dataset we used"). In general, answering "[No]" or "[NA]" is not grounds for rejection. While the questions are phrased in a binary way, we acknowledge that the true answer is often more nuanced, so please just use your best judgment and write a justification to elaborate. All supporting evidence can appear either in the main paper or the supplemental material, provided in appendix. If you answer [Yes] to a question, in the justification please point to the section(s) where related material for the question can be found.

IMPORTANT, please:

- **Delete this instruction block, but keep the section heading "NeurIPS Paper Checklist",**
- **Keep the checklist subsection headings, questions/answers and guidelines below.**
- **Do not modify the questions and only use the provided macros for your answers.**

1. Claims

Question: Do the main claims made in the abstract and introduction accurately reflect the paper's contributions and scope?

Answer: [Yes]

Justification: The main claims made in the abstract and introduction accurately reflect the paper's contributions and scope. The method can be found in Section C.6 and 4. Experimental results are illustrated in Section 5. The detailed proofs and experimental settings can be found in the Appendix.

Guidelines:

- The answer NA means that the abstract and introduction do not include the claims made in the paper.
- The abstract and/or introduction should clearly state the claims made, including the contributions made in the paper and important assumptions and limitations. A No or NA answer to this question will not be perceived well by the reviewers.
- The claims made should match theoretical and experimental results, and reflect how much the results can be expected to generalize to other settings.
- It is fine to include aspirational goals as motivation as long as it is clear that these goals are not attained by the paper.

2. Limitations

Question: Does the paper discuss the limitations of the work performed by the authors?

Answer: [Yes]

Justification: We include the limitations in our conclusion. We leave this part as our future work.

Guidelines:

- The answer NA means that the paper has no limitation while the answer No means that the paper has limitations, but those are not discussed in the paper.
- The authors are encouraged to create a separate "Limitations" section in their paper.
- The paper should point out any strong assumptions and how robust the results are to violations of these assumptions (e.g., independence assumptions, noiseless settings, model well-specification, asymptotic approximations only holding locally). The authors should reflect on how these assumptions might be violated in practice and what the implications would be.
- The authors should reflect on the scope of the claims made, e.g., if the approach was only tested on a few datasets or with a few runs. In general, empirical results often depend on implicit assumptions, which should be articulated.
- The authors should reflect on the factors that influence the performance of the approach. For example, a facial recognition algorithm may perform poorly when image resolution is low or images are taken in low lighting. Or a speech-to-text system might not be used reliably to provide closed captions for online lectures because it fails to handle technical jargon.
- The authors should discuss the computational efficiency of the proposed algorithms and how they scale with dataset size.
- If applicable, the authors should discuss possible limitations of their approach to address problems of privacy and fairness.
- While the authors might fear that complete honesty about limitations might be used by reviewers as grounds for rejection, a worse outcome might be that reviewers discover limitations that aren't acknowledged in the paper. The authors should use their best judgment and recognize that individual actions in favor of transparency play an important role in developing norms that preserve the integrity of the community. Reviewers will be specifically instructed to not penalize honesty concerning limitations.

3. Theory assumptions and proofs

Question: For each theoretical result, does the paper provide the full set of assumptions and a complete (and correct) proof?

Answer: [Yes]

Justification: We have provided the full set of assumptions and corresponding complete proofs under each proposed Theorem with detailed derivations included in the Appendix B.

Guidelines:

- The answer NA means that the paper does not include theoretical results.
- All the theorems, formulas, and proofs in the paper should be numbered and cross-referenced.
- All assumptions should be clearly stated or referenced in the statement of any theorems.
- The proofs can either appear in the main paper or the supplemental material, but if they appear in the supplemental material, the authors are encouraged to provide a short proof sketch to provide intuition.
- Inversely, any informal proof provided in the core of the paper should be complemented by formal proofs provided in appendix or supplemental material.
- Theorems and Lemmas that the proof relies upon should be properly referenced.

4. Experimental result reproducibility

Question: Does the paper fully disclose all the information needed to reproduce the main experimental results of the paper to the extent that it affects the main claims and/or conclusions of the paper (regardless of whether the code and data are provided or not)?

Answer: [Yes]

Justification: In addition to the description in the paper, we included more detailed hyperparameters settings in the Appendix.

Guidelines:

- The answer NA means that the paper does not include experiments.
- If the paper includes experiments, a No answer to this question will not be perceived well by the reviewers: Making the paper reproducible is important, regardless of whether the code and data are provided or not.
- If the contribution is a dataset and/or model, the authors should describe the steps taken to make their results reproducible or verifiable.
- Depending on the contribution, reproducibility can be accomplished in various ways. For example, if the contribution is a novel architecture, describing the architecture fully might suffice, or if the contribution is a specific model and empirical evaluation, it may be necessary to either make it possible for others to replicate the model with the same dataset, or provide access to the model. In general, releasing code and data is often one good way to accomplish this, but reproducibility can also be provided via detailed instructions for how to replicate the results, access to a hosted model (e.g., in the case of a large language model), releasing of a model checkpoint, or other means that are appropriate to the research performed.
- While NeurIPS does not require releasing code, the conference does require all submissions to provide some reasonable avenue for reproducibility, which may depend on the nature of the contribution. For example
 - (a) If the contribution is primarily a new algorithm, the paper should make it clear how to reproduce that algorithm.
 - (b) If the contribution is primarily a new model architecture, the paper should describe the architecture clearly and fully.
 - (c) If the contribution is a new model (e.g., a large language model), then there should either be a way to access this model for reproducing the results or a way to reproduce the model (e.g., with an open-source dataset or instructions for how to construct the dataset).
 - (d) We recognize that reproducibility may be tricky in some cases, in which case authors are welcome to describe the particular way they provide for reproducibility. In the case of closed-source models, it may be that access to the model is limited in some way (e.g., to registered users), but it should be possible for other researchers to have some path to reproducing or verifying the results.

5. Open access to data and code

Question: Does the paper provide open access to the data and code, with sufficient instructions to faithfully reproduce the main experimental results, as described in supplemental material?

Answer: [No]

Justification: The model architecture and hyperparameter settings are all included in this work. We believe we have provided enough details. We will make the code available in the near future.

Guidelines:

- The answer NA means that paper does not include experiments requiring code.
- Please see the NeurIPS code and data submission guidelines (<https://nips.cc/public/guides/CodeSubmissionPolicy>) for more details.
- While we encourage the release of code and data, we understand that this might not be possible, so “No” is an acceptable answer. Papers cannot be rejected simply for not including code, unless this is central to the contribution (e.g., for a new open-source benchmark).
- The instructions should contain the exact command and environment needed to run to reproduce the results. See the NeurIPS code and data submission guidelines (<https://nips.cc/public/guides/CodeSubmissionPolicy>) for more details.
- The authors should provide instructions on data access and preparation, including how to access the raw data, preprocessed data, intermediate data, and generated data, etc.

- The authors should provide scripts to reproduce all experimental results for the new proposed method and baselines. If only a subset of experiments are reproducible, they should state which ones are omitted from the script and why.
- At submission time, to preserve anonymity, the authors should release anonymized versions (if applicable).
- Providing as much information as possible in supplemental material (appended to the paper) is recommended, but including URLs to data and code is permitted.

6. Experimental setting/details

Question: Does the paper specify all the training and test details (e.g., data splits, hyper-parameters, how they were chosen, type of optimizer, etc.) necessary to understand the results?

Answer: [\[Yes\]](#)

Justification: The details are included in Appendix.

Guidelines:

- The answer NA means that the paper does not include experiments.
- The experimental setting should be presented in the core of the paper to a level of detail that is necessary to appreciate the results and make sense of them.
- The full details can be provided either with the code, in appendix, or as supplemental material.

7. Experiment statistical significance

Question: Does the paper report error bars suitably and correctly defined or other appropriate information about the statistical significance of the experiments?

Answer: [\[Yes\]](#)

Justification: For every experiment introduced, we run with multiple random seeds and reported both mean and std averaged over these multiple random seeds.

Guidelines:

- The answer NA means that the paper does not include experiments.
- The authors should answer "Yes" if the results are accompanied by error bars, confidence intervals, or statistical significance tests, at least for the experiments that support the main claims of the paper.
- The factors of variability that the error bars are capturing should be clearly stated (for example, train/test split, initialization, random drawing of some parameter, or overall run with given experimental conditions).
- The method for calculating the error bars should be explained (closed form formula, call to a library function, bootstrap, etc.)
- The assumptions made should be given (e.g., Normally distributed errors).
- It should be clear whether the error bar is the standard deviation or the standard error of the mean.
- It is OK to report 1-sigma error bars, but one should state it. The authors should preferably report a 2-sigma error bar than state that they have a 96% CI, if the hypothesis of Normality of errors is not verified.
- For asymmetric distributions, the authors should be careful not to show in tables or figures symmetric error bars that would yield results that are out of range (e.g. negative error rates).
- If error bars are reported in tables or plots, The authors should explain in the text how they were calculated and reference the corresponding figures or tables in the text.

8. Experiments compute resources

Question: For each experiment, does the paper provide sufficient information on the computer resources (type of compute workers, memory, time of execution) needed to reproduce the experiments?

Answer: [\[Yes\]](#)

Justification: As mentioned in Appendix, our model runs on an NVIDIA RTX 3080TI GPU and an Intel i9-12900k CPU.

Guidelines:

- The answer NA means that the paper does not include experiments.
- The paper should indicate the type of compute workers CPU or GPU, internal cluster, or cloud provider, including relevant memory and storage.
- The paper should provide the amount of compute required for each of the individual experimental runs as well as estimate the total compute.
- The paper should disclose whether the full research project required more compute than the experiments reported in the paper (e.g., preliminary or failed experiments that didn't make it into the paper).

9. Code of ethics

Question: Does the research conducted in the paper conform, in every respect, with the NeurIPS Code of Ethics <https://neurips.cc/public/EthicsGuidelines?>

Answer: [Yes]

Justification: We are strictly following NeurIPS Code of Ethics.

Guidelines:

- The answer NA means that the authors have not reviewed the NeurIPS Code of Ethics.
- If the authors answer No, they should explain the special circumstances that require a deviation from the Code of Ethics.
- The authors should make sure to preserve anonymity (e.g., if there is a special consideration due to laws or regulations in their jurisdiction).

10. Broader impacts

Question: Does the paper discuss both potential positive societal impacts and negative societal impacts of the work performed?

Answer: [NA]

Justification: Our paper proposes a novel method for MARL, and we do not think there would be any direct social impact of it.

Guidelines:

- The answer NA means that there is no societal impact of the work performed.
- If the authors answer NA or No, they should explain why their work has no societal impact or why the paper does not address societal impact.
- Examples of negative societal impacts include potential malicious or unintended uses (e.g., disinformation, generating fake profiles, surveillance), fairness considerations (e.g., deployment of technologies that could make decisions that unfairly impact specific groups), privacy considerations, and security considerations.
- The conference expects that many papers will be foundational research and not tied to particular applications, let alone deployments. However, if there is a direct path to any negative applications, the authors should point it out. For example, it is legitimate to point out that an improvement in the quality of generative models could be used to generate deepfakes for disinformation. On the other hand, it is not needed to point out that a generic algorithm for optimizing neural networks could enable people to train models that generate Deepfakes faster.
- The authors should consider possible harms that could arise when the technology is being used as intended and functioning correctly, harms that could arise when the technology is being used as intended but gives incorrect results, and harms following from (intentional or unintentional) misuse of the technology.
- If there are negative societal impacts, the authors could also discuss possible mitigation strategies (e.g., gated release of models, providing defenses in addition to attacks, mechanisms for monitoring misuse, mechanisms to monitor how a system learns from feedback over time, improving the efficiency and accessibility of ML).

11. Safeguards

Question: Does the paper describe safeguards that have been put in place for responsible release of data or models that have a high risk for misuse (e.g., pretrained language models, image generators, or scraped datasets)?

Answer: [NA]

Justification: The paper poses no such risks.

Guidelines:

- The answer NA means that the paper poses no such risks.
- Released models that have a high risk for misuse or dual-use should be released with necessary safeguards to allow for controlled use of the model, for example by requiring that users adhere to usage guidelines or restrictions to access the model or implementing safety filters.
- Datasets that have been scraped from the Internet could pose safety risks. The authors should describe how they avoided releasing unsafe images.
- We recognize that providing effective safeguards is challenging, and many papers do not require this, but we encourage authors to take this into account and make a best faith effort.

12. Licenses for existing assets

Question: Are the creators or original owners of assets (e.g., code, data, models), used in the paper, properly credited and are the license and terms of use explicitly mentioned and properly respected?

Answer: [Yes]

Justification: We cited all the creators or original owners of assets mentioned in the paper.

Guidelines:

- The answer NA means that the paper does not use existing assets.
- The authors should cite the original paper that produced the code package or dataset.
- The authors should state which version of the asset is used and, if possible, include a URL.
- The name of the license (e.g., CC-BY 4.0) should be included for each asset.
- For scraped data from a particular source (e.g., website), the copyright and terms of service of that source should be provided.
- If assets are released, the license, copyright information, and terms of use in the package should be provided. For popular datasets, paperswithcode.com/datasets has curated licenses for some datasets. Their licensing guide can help determine the license of a dataset.
- For existing datasets that are re-packaged, both the original license and the license of the derived asset (if it has changed) should be provided.
- If this information is not available online, the authors are encouraged to reach out to the asset's creators.

13. New assets

Question: Are new assets introduced in the paper well documented and is the documentation provided alongside the assets?

Answer: [NA]

Justification: The paper does not release new assets.

Guidelines:

- The answer NA means that the paper does not release new assets.
- Researchers should communicate the details of the dataset/code/model as part of their submissions via structured templates. This includes details about training, license, limitations, etc.
- The paper should discuss whether and how consent was obtained from people whose asset is used.
- At submission time, remember to anonymize your assets (if applicable). You can either create an anonymized URL or include an anonymized zip file.

14. Crowdsourcing and research with human subjects

Question: For crowdsourcing experiments and research with human subjects, does the paper include the full text of instructions given to participants and screenshots, if applicable, as well as details about compensation (if any)?

Answer: [NA]

Justification: The paper does not involve crowdsourcing nor research with human subjects.

Guidelines:

- The answer NA means that the paper does not involve crowdsourcing nor research with human subjects.
- Including this information in the supplemental material is fine, but if the main contribution of the paper involves human subjects, then as much detail as possible should be included in the main paper.
- According to the NeurIPS Code of Ethics, workers involved in data collection, curation, or other labor should be paid at least the minimum wage in the country of the data collector.

15. Institutional review board (IRB) approvals or equivalent for research with human subjects

Question: Does the paper describe potential risks incurred by study participants, whether such risks were disclosed to the subjects, and whether Institutional Review Board (IRB) approvals (or an equivalent approval/review based on the requirements of your country or institution) were obtained?

Answer: [NA]

Justification: The paper does not involve crowdsourcing nor research with human subjects.

Guidelines:

- The answer NA means that the paper does not involve crowdsourcing nor research with human subjects.
- Depending on the country in which research is conducted, IRB approval (or equivalent) may be required for any human subjects research. If you obtained IRB approval, you should clearly state this in the paper.
- We recognize that the procedures for this may vary significantly between institutions and locations, and we expect authors to adhere to the NeurIPS Code of Ethics and the guidelines for their institution.
- For initial submissions, do not include any information that would break anonymity (if applicable), such as the institution conducting the review.

16. Declaration of LLM usage

Question: Does the paper describe the usage of LLMs if it is an important, original, or non-standard component of the core methods in this research? Note that if the LLM is used only for writing, editing, or formatting purposes and does not impact the core methodology, scientific rigor, or originality of the research, declaration is not required.

Answer: [NA]

Justification: The core method development in this research does not involve LLMs as any important, original, or non-standard components.

Guidelines:

- The answer NA means that the core method development in this research does not involve LLMs as any important, original, or non-standard components.
- Please refer to our LLM policy (<https://neurips.cc/Conferences/2025/LLM>) for what should or should not be described.